Vector meson photoproduction in ALICE at the LHC

Adam Matyja

Institute of Nuclear Physics
Polish Academy of Sciences, Kraków

UJ Particle Physics
Phenomenology and Experiments Seminar

24 Oct 2022 - Kraków

Outline

- Introduction
- ALICE detector
- Mesurements
  - ρ^0 photoproduction in Pb-Pb and Xe-Xe
  - J/ψ and ψ' photoproduction in Pb-Pb
  - $\mu^+\mu^-$ pair production and J/ψ photoproduction in p-Pb
- Detector upgrade
- Run 3 and beyond perspectives
  - Anomalous magnetic moment of τ lepton
  - Light-by-light scattering
- Summary

Ultra-peripheral collisions (UPC)

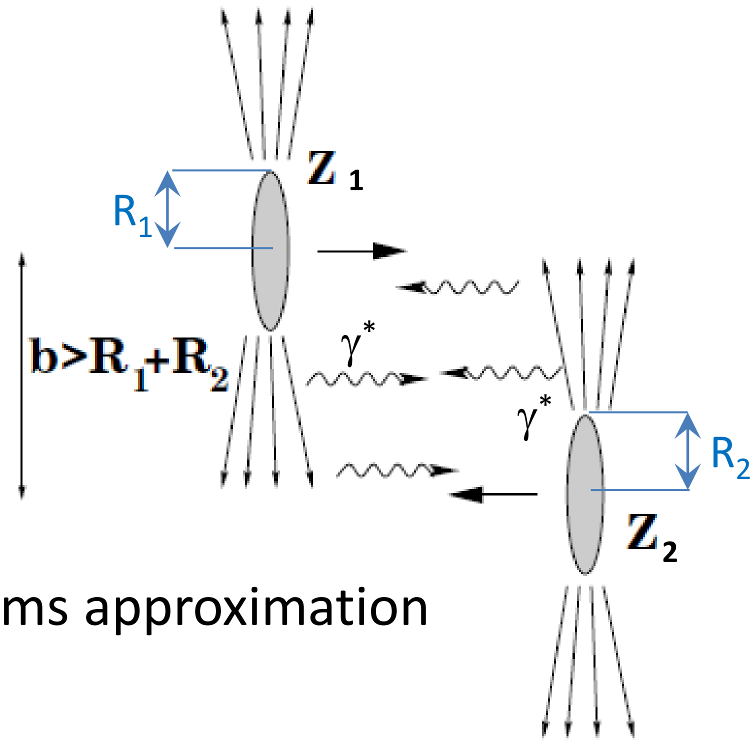

- Impact parameter $b > R_1 + R_2$
  - Hadronic interactions suppressed
- Photon induced reactions:
  - Well described in Weizsäcker-Williams approximation
  - Photon flux ~ Z^2 (Z_{Pb} = 82)
  - Large γ-induced interaction cross section
- Clear signature - rapidity gap(s)

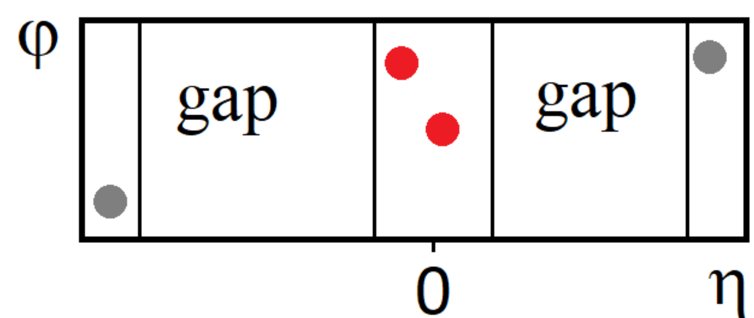

Photon induced processes

- Photon – hadron interactions

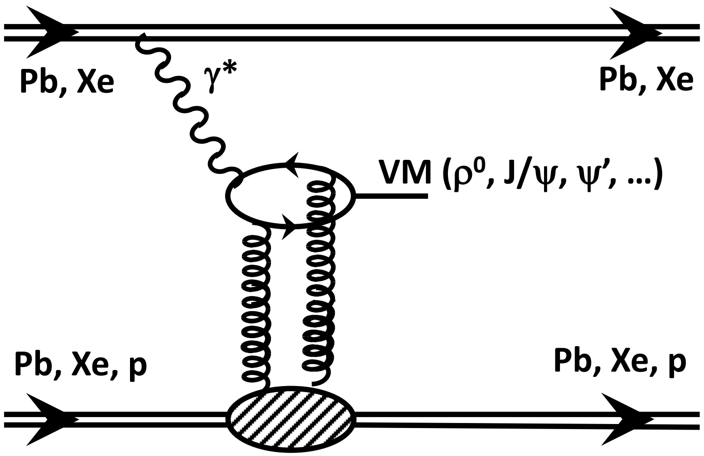

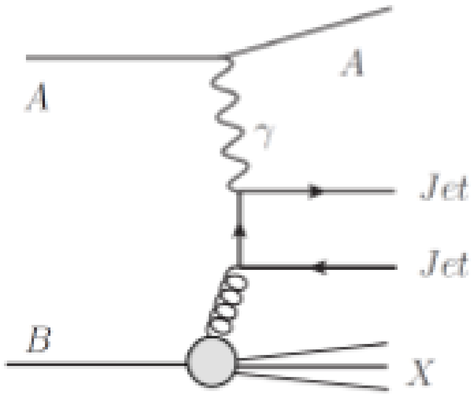

- Photon – photon interactions

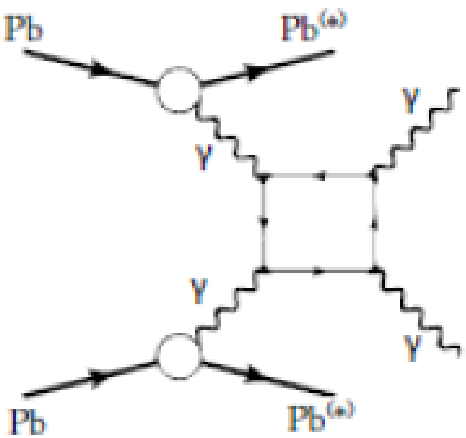

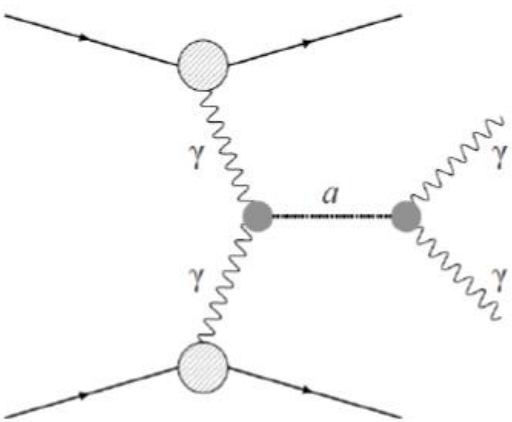

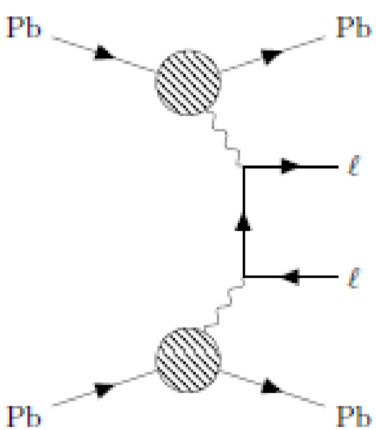

Impact parameter dependence

No breakup (0n0n)

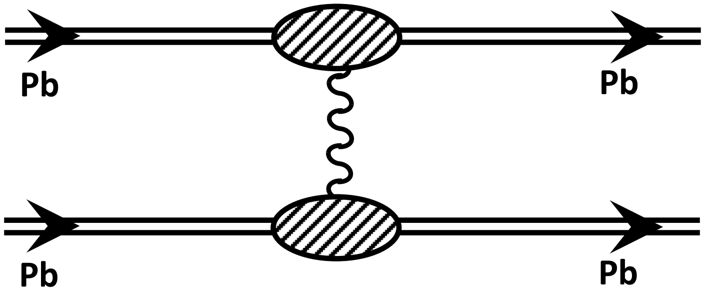

Single breakup (Xn0n + 0nXn)

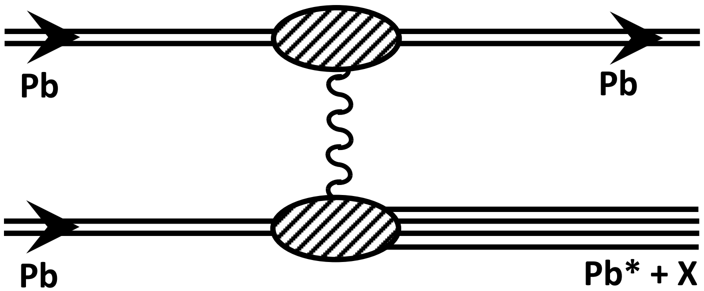

Double breakup (XnXn)

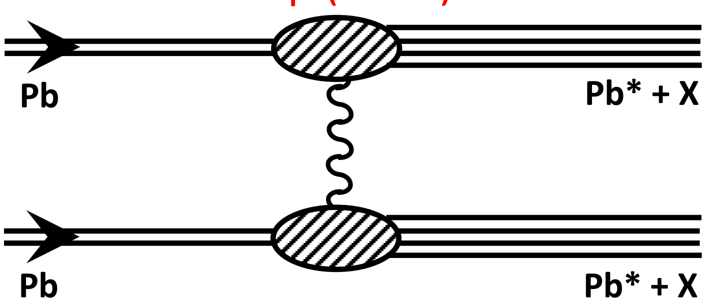

- Excitation of the nuclei possible through the secondary photon exchange

⇒ Giant dipole resonance

All protons vibrating against all neutrons → Knocks out 1-4 neutrons

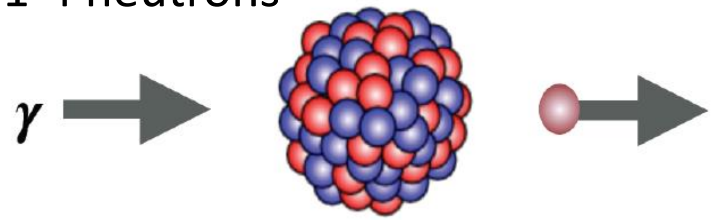

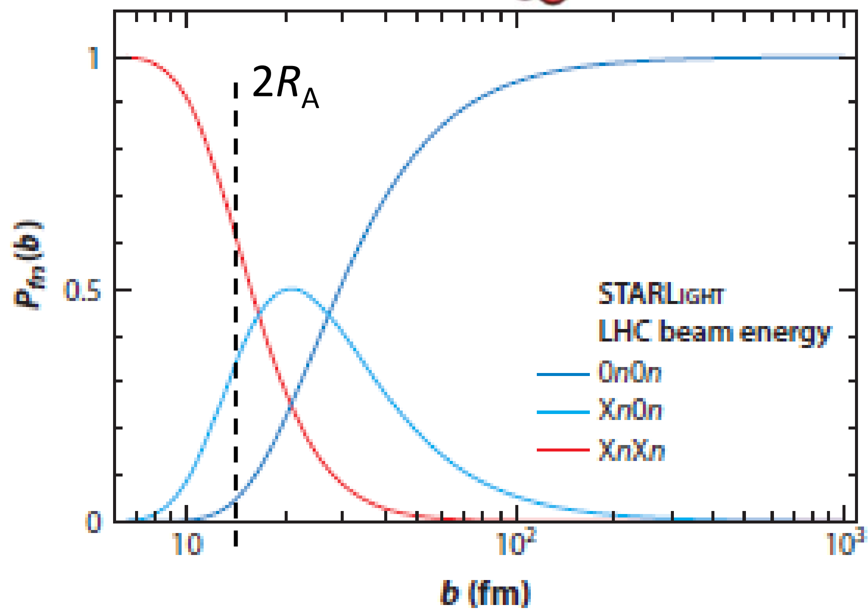

S. Klein, P. Steinberg, Annu. Rev. Nucl. Part. Sci. 70(1), 323 (2020)

UPC event clasifier: 0n0n, 0nXn, XnXn

→ via electromagnetic dissociation (EMD)

Photoproduction and main variables

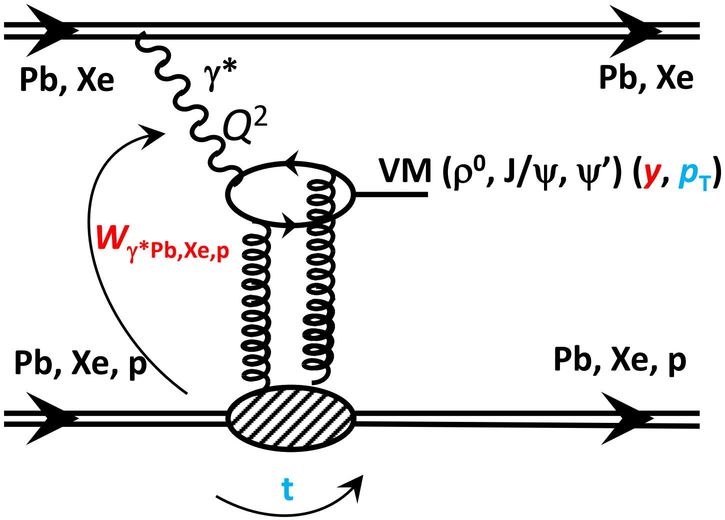

Ryskin: Z. Phys. C 57, 89-92 (1993)

$$\frac{d\sigma^T(\gamma p \to J/\Psi + p)}{dt} = \frac{|M|^2}{16\pi s^2}$$

$$= |F_N^{2G}(t)|^2 \frac{\alpha_s^2 \Gamma_{ee}^J m_J^3}{3\alpha_{e.m.}} \pi^3 \left[\bar{x} G(\bar{x}, \bar{q}^2) \frac{2\bar{q}^2 - |q_t^J|^2}{(2\bar{q}^2)^3} \right]^2$$

- Photon virtuality $Q^2 \sim M_{VM}^2 / 4$
- Vector Meson (VM) quantum numbers:
  - $J^{PC} = 1^{--}$
- Bjorken-x

$$x_B = \frac{M_{VM}}{\sqrt{s_{NN}}} e^{\pm y}$$

  - ➢ Photoproduction is sensitive to the x_B evolution at LO of the gluon distribution (nPDFs)
- Photon-target centre-of-mass energy

$$W^2_{\gamma^* Pb,Xe,p} = 2E_{Pb,Xe,p} M_{VM} e^{\mp y}$$

- 4-momentum transfer t
  - Transverse plain gluon distribution $|t| \sim p_T^2$

Photoproduction and main variables

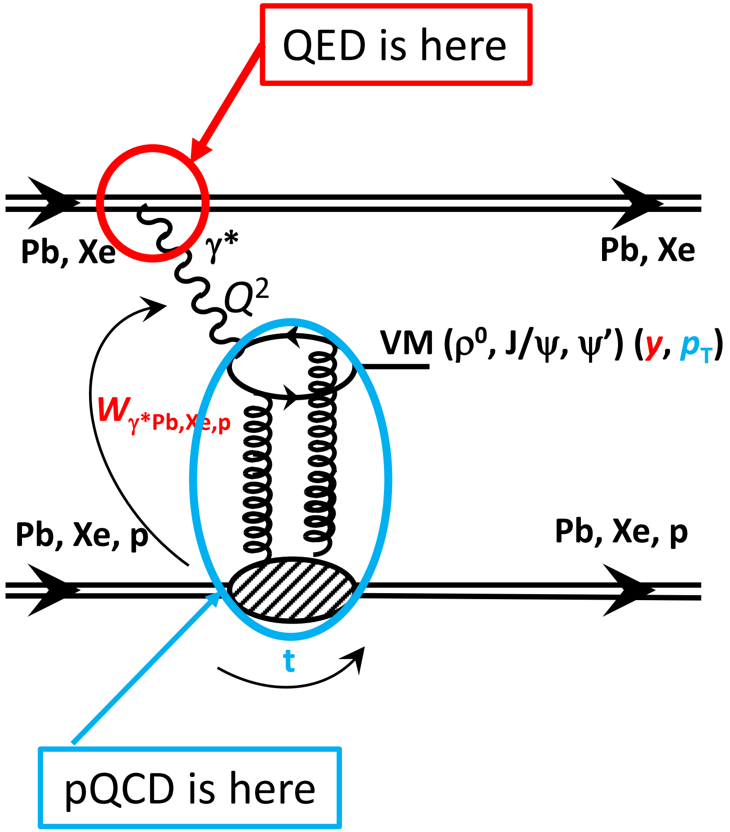

- Photon virtuality $Q^2 \sim M_{VM}^2 / 4$
- Vector Meson (VM) quantum numbers:
  - $J^{PC} = 1^{--}$
- Bjorken-x

$$x_B = \frac{M_{VM}}{\sqrt{s_{NN}}} e^{\pm y}$$

  - ➢ Photoproduction is sensitive to the x_B evolution at LO of the gluon distribution (nPDFs)
- Photon-target centre-of-mass energy

$$W^2_{\gamma^* Pb,Xe,p} = 2E_{Pb,Xe,p} M_{VM} e^{\mp y}$$

- 4-momentum transfer t
  - Transverse plain gluon distribution $|t| \sim p_T^2$

p_T signature

- **Coherent** Vector Meson (VM) photoproduction:
  - Photon couples coherently to all nucleons (whole nucleus)
  - $\langle p_T^{VM} \rangle \sim 1/R_{Pb} \sim 50$ MeV/c
  - Target ion stays intact

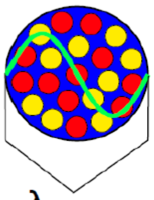

- **Incoherent** VM photoproduction:
  - Photon couples to a single nucleon
  - $\langle p_T^{VM} \rangle \sim 1/R_p \sim 400$ MeV/c
  - Target ion breaks, nucleon stays intact
  - Usually accompanied by neutron emission

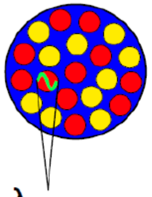

- **Exclusive** VM photoproduction:
  - Photon couples to a single nucleon (proton)
  - $\langle p_T^{VM} \rangle \sim 1/R_p \sim 400$ MeV/c
  - Target proton stays intact (similar to coherent) in p-Pb case
- **Dissociative** VM photoproduction:
  - Photon interacts with a single nucleon and excites it
  - $\langle p_T^{VM} \rangle \sim 1$ GeV/c
  - Target nucleon and ion break (in heavy ion collision)
  - Target proton breaks (in p-Pb)

Motivation

- Coherent vector meson (ρ^0, J/ψ, ψ') photoproduction allows for the study of (gluon) shadowing and atomic number *A* dependence
- Heavy VMs particularly sensitive to gluon shadowing
  - Nuclear gluon shadowing factor $R_g^A(x,Q^2)=g_A(x,Q^2)/Ag_p(x,Q^2) < 1$
  - Saturation may contribute to nuclear shadowing
  - Search for saturation at low x_B
- $|t|$-dependence helps to constrain transverse gluonic structure at low x_B
- Large photonuclear production cross section of ρ^0 meson allows for studies of black-disk limit of QCD approach
- How well do we model photon flux?
- Coupling at the vertex is large ($Z\alpha \sim 0.6$) $\Rightarrow$ do we need NLO corrections?
- Constrain parameters of models

Accardi et. al.: Eur.Phys.J.A 52 (2016) 9, 268

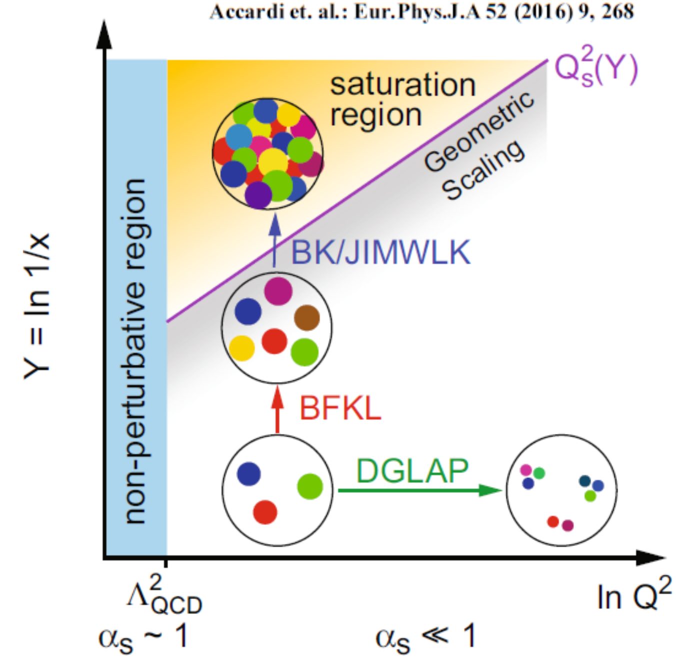

Eskola et. al.: Eur.Phys.J.C 77 (2017) 3, 163

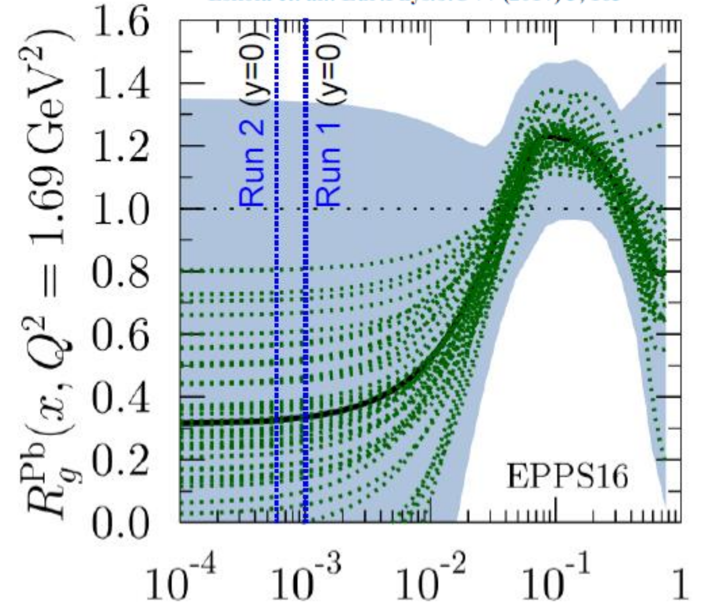

ALICE detector

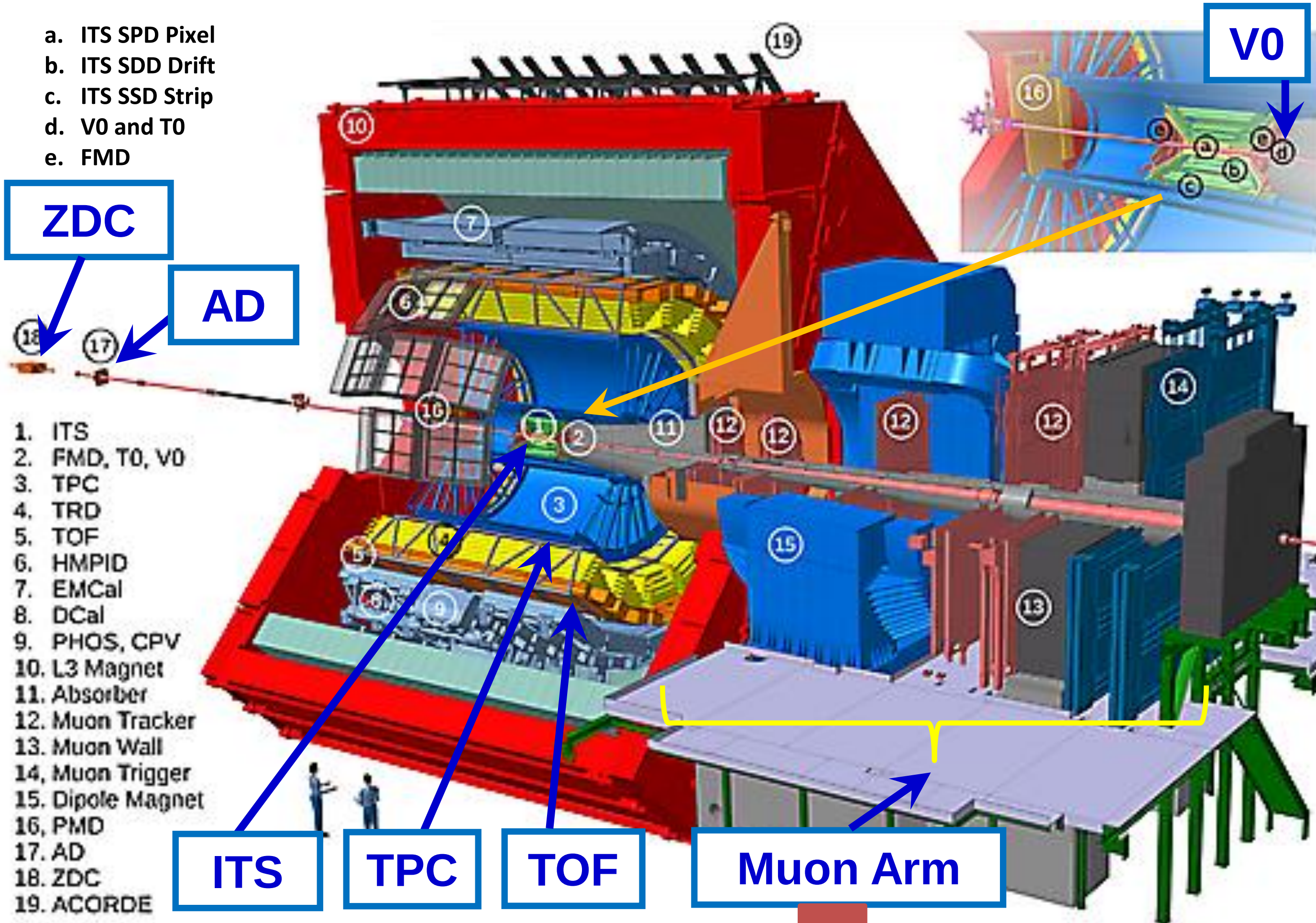

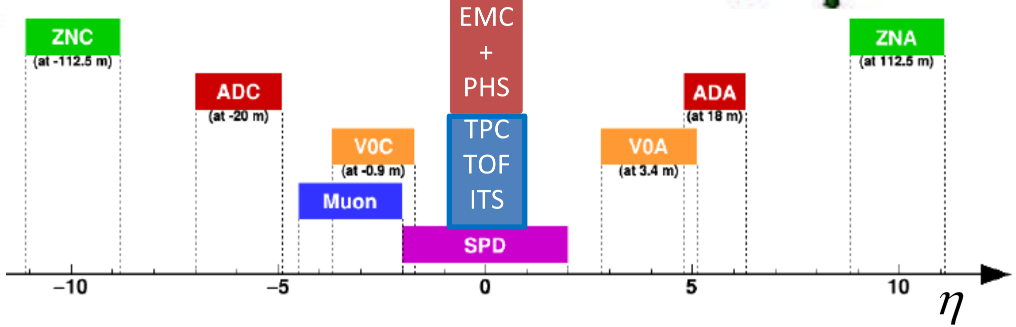

- Central Barrel tracking ($e^{\pm}$, $h^{\pm}$)
  - $|\eta| < 0.9$, $0 < \varphi < 2\pi$
  - ITS - silicon detector
  - TPC - gas drift detector
  - TOF - resistive plate chambers
- Forward tracking ($\mu^{\pm}$)
  - $-4 < \eta < -2.5$
  - Absorber
  - Muon tracker
  - Muon trigger
  - Dipole magnet
- Diffractive detectors
  - AD - scintillator counter
  - V0 - scintillator counter
  - ZDC - sampling calorimeter

Vertex
- Pixel

Trigger
- SPD, TOF, AD, V0, Muon

ρ^0 in Pb-Pb at $\sqrt{s_{NN}}$ = 5.02 TeV

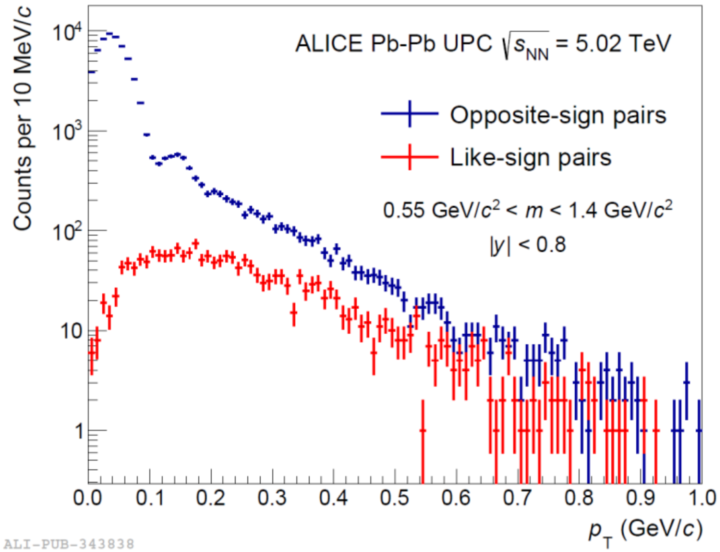

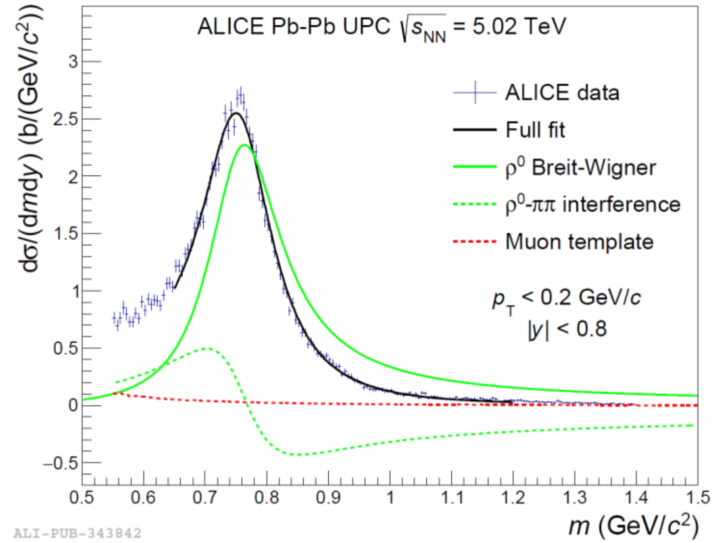

JHEP 06 (2020) 035

$$\frac{d\sigma}{dm\,dy} = |A \cdot BW_\rho + B|^2 + M,$$

$$BW_\rho = \frac{\sqrt{m \cdot m_{\rho^0} \cdot \Gamma(m)}}{m^2 - m_{\rho^0}^2 + i m_{\rho^0} \cdot \Gamma(m)} \qquad \Gamma(m) = \Gamma(m_{\rho^0}) \cdot \frac{m_{\rho^0}}{m} \cdot \left(\frac{m^2 - 4m_\pi^2}{m_{\rho^0}^2 - m_\pi^2}\right)^{3/2}$$

- Coherent $\rho^0 \rightarrow \pi^+\pi^-$
  - Pole mass 769.5 ± 1.2^{stat} ± 2.0^{syst} MeV/c^2
  - width 156 ± 2^{stat} ± 3^{syst} MeV/c^2
  - agree with PDG
  - Large cross section ~550 mb

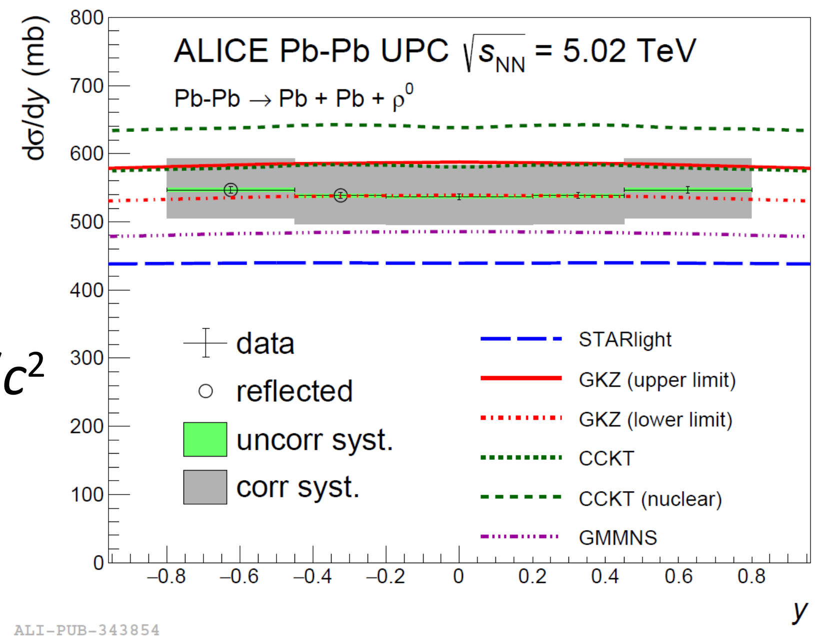

ρ^0 in Pb-Pb at $\sqrt{s_{NN}}$ = 5.02 TeV

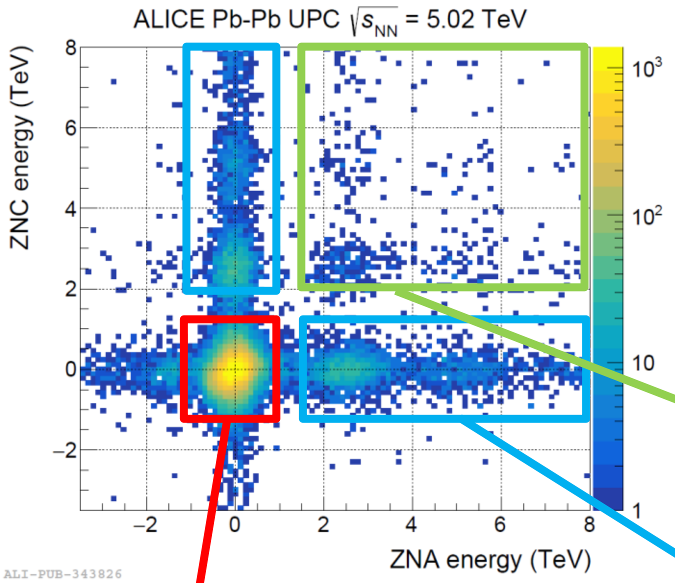

- Impact parameter dependence via ZDC selection in 3 classes: 0n0n, 0nXn, XnXn
- Comparisons with models
  - GKZ (nuclear shadowing) gives the best description
  - CCKT (saturation) is slightly worse
  - STARlight and GMMNS (saturation) underestimate
- Test of photon flux description

JHEP 06 (2020) 035

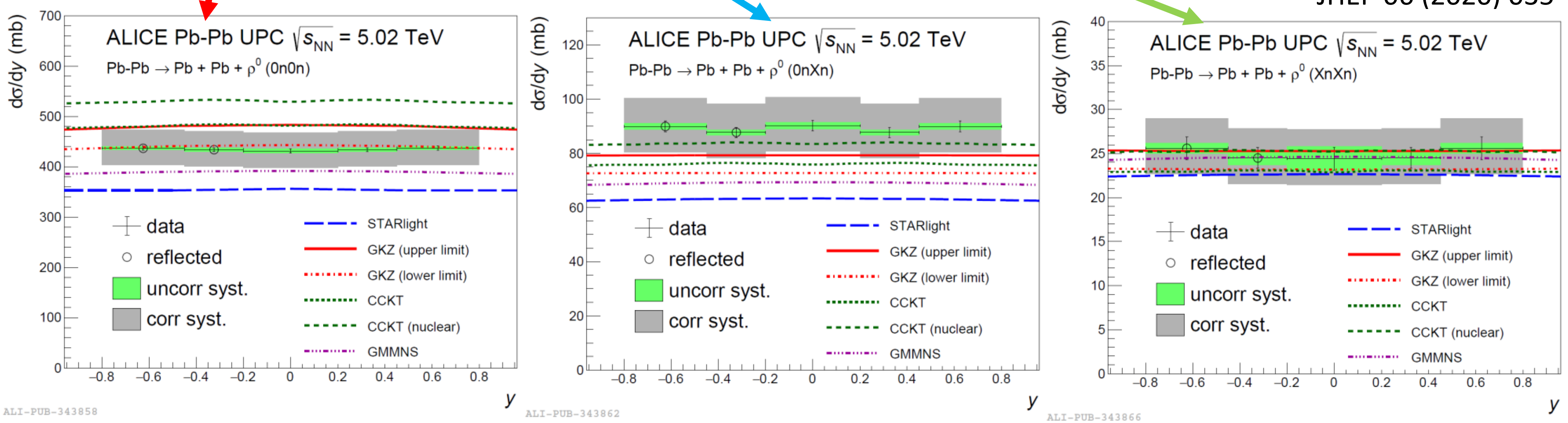

ρ′ in Pb-Pb at $\sqrt{s_{NN}}$ = 5.02 TeV

- Resonance-like structure $M^{\pi\pi} \sim 1.7$ GeV/c^2
  - Significance of 4.5 σ
  - Seen also by STAR, ZEUS, H1
  - Most probably ρ_3(1690) with angular momrentum J = 3

$$\frac{dN_{\pi\pi}}{dm} = P_1 \cdot \exp(-P_2 \cdot (m - 1.2\,\mathrm{GeV/c^2})) + P_3 + P_4 \cdot \exp(-(m - M_x)^2/\Gamma_x^2)$$

JHEP 06 (2020) 035

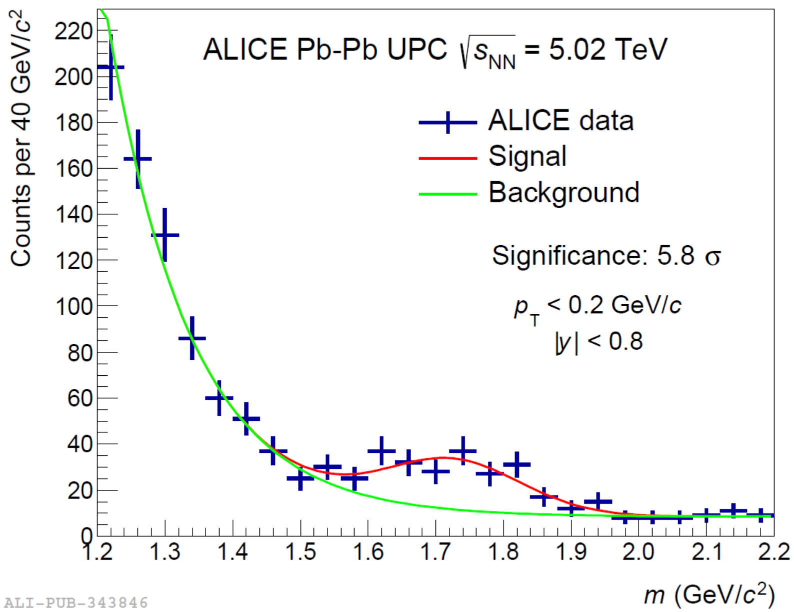

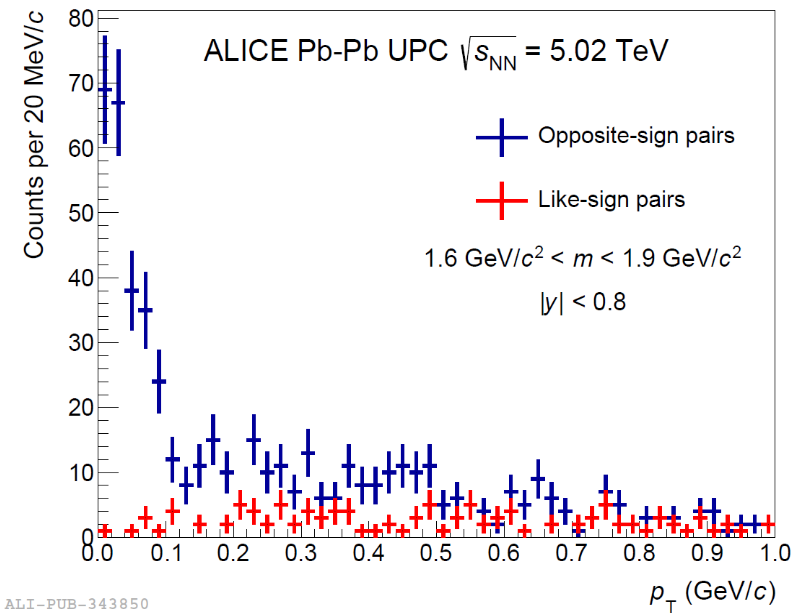

ρ^0 in Xe-Xe at $\sqrt{s_{NN}} = 5.44$ TeV

- $d\sigma/dy = 131.5 \pm 5.6^{st} {}^{+17.5}_{-16.9}{}^{sy}$ mb
- All models relatively close to data

- $W_{\gamma A,n} = 65$ GeV
- $\sigma(\gamma A \rightarrow \rho^0 A) \sim A^{\alpha}$ with a slope $\alpha = 0.96 \pm 0.02^{sy}$
  - $\Rightarrow$ Signals important shadowing effect
  - – Far from black disk limit
  - – Slope close to 1 by coincidence
- Fair description of data by models CCKT (saturation) and GKZ (shadowing)

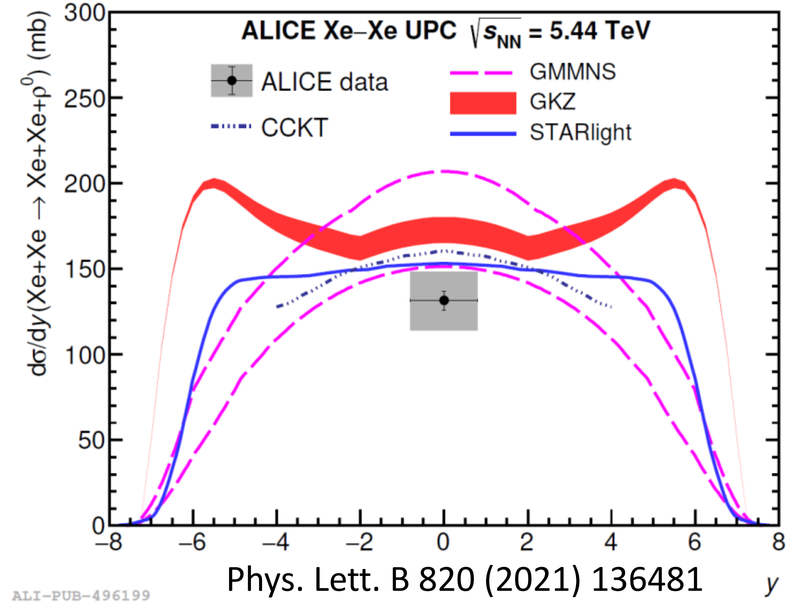

Phys. Lett. B 820 (2021) 136481

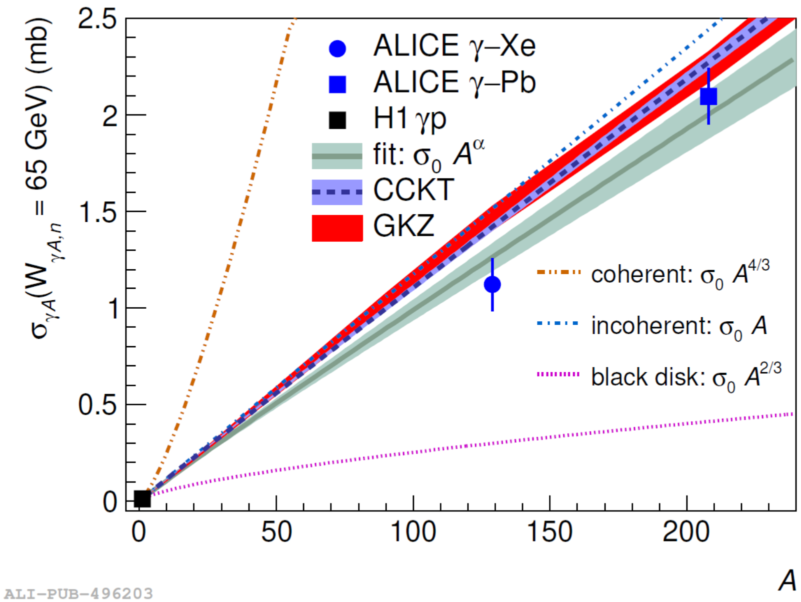

J/ψ in Pb-Pb at $\sqrt{s_{NN}}$ = 5.02 TeV

- Forward region:
  - $J/\psi \rightarrow \mu^+\mu^-$
- Central region:
  - $J/\psi \rightarrow \mu^+\mu^-$, e^+e^-, $p\bar{p}$
- Nuclear gluon shadowing factor $R_g = 0.64 \pm 0.04$ for $0.3 \times 10^{-3} < x_B < 1.4 \times 10^{-3}$
- No model describes the full rapidity dependence
  - Models with nuclear shadowing (EPS09 LO, LTA) or saturation (GG-HS) describe central and very forward data but tensions in semiforward region
  - Other models describe either forward or central rapidity region

Eur. Phys. J. C 81 (2021) 712

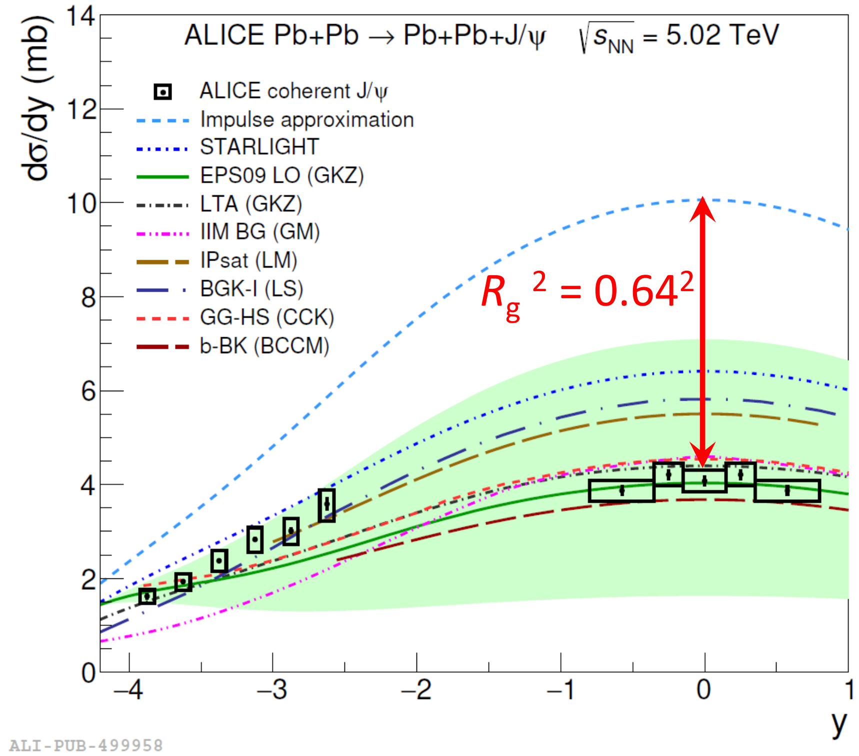

Rapidity dependance: Ambiguity problem

- Two sources $\Rightarrow$ two values of x_B

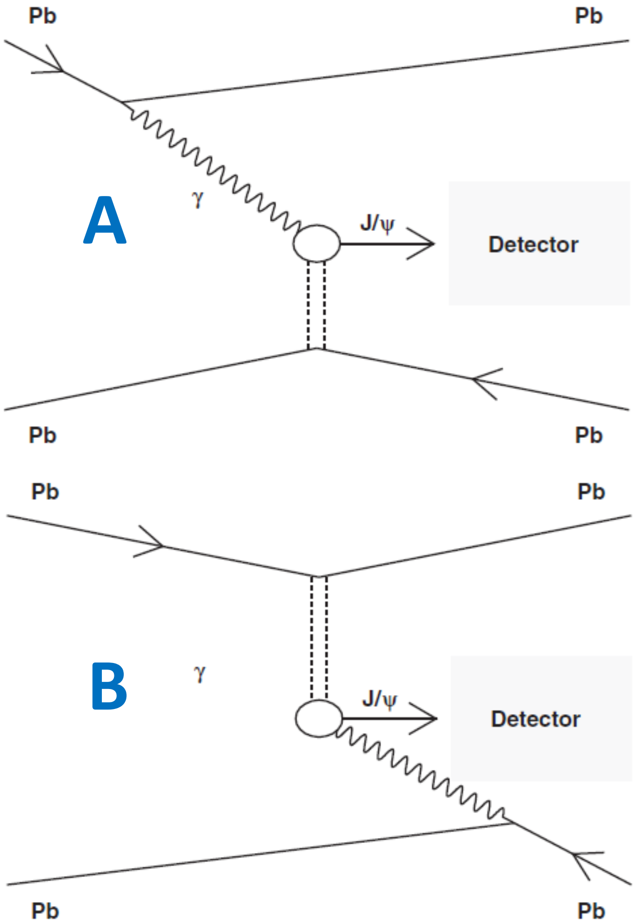

J. G. Contreras, PRC 96, 015203 (2017)

Eur. Phys. J. C 81 (2021) 712

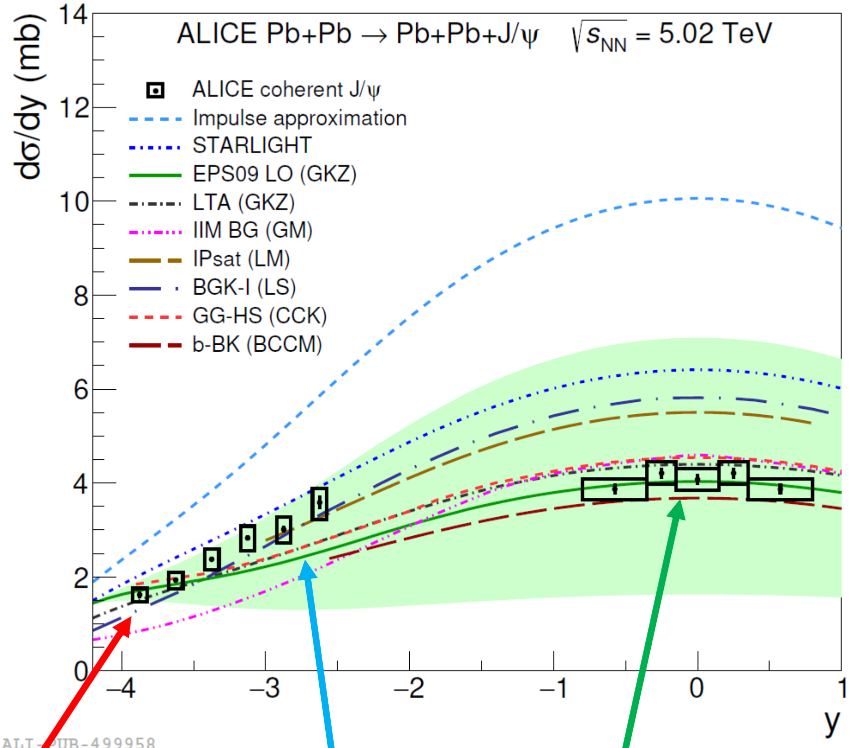

A: 5 % $x_B \sim 1.1 \times 10^{-5}$
B: 95 % $x_B \sim 3.3 \times 10^{-2}$

50 % each $x_B \sim 10^{-3}$

A: 40 % $x_B \sim 5.1 \times 10^{-4}$
B: 60 % $x_B \sim 0.7 \times 10^{-2}$

To disentangle both contributions we need to measure the same proces with EMD or in peripheral collisions

ψ' in Pb-Pb at $\sqrt{s_{NN}} = 5.02$ TeV

- $\psi' \to \mu^+\mu^-\pi^+\pi^-$, $e^+e^-\pi^+\pi^-$, l^+l^-
- Nuclear gluon shadowing factor
  - $R_g = 0.66 \pm 0.06$ for $0.3 \times 10^{-3} < x_B < 1.4 \times 10^{-3}$
  - Consistent with J/ψ result
- Good agreement of models with shadowing (EPS09 LO, LTA)
- Good agreement of model BCCM with saturation
- Other models overpredict data

Eur. Phys. J. C 81 (2021) 712

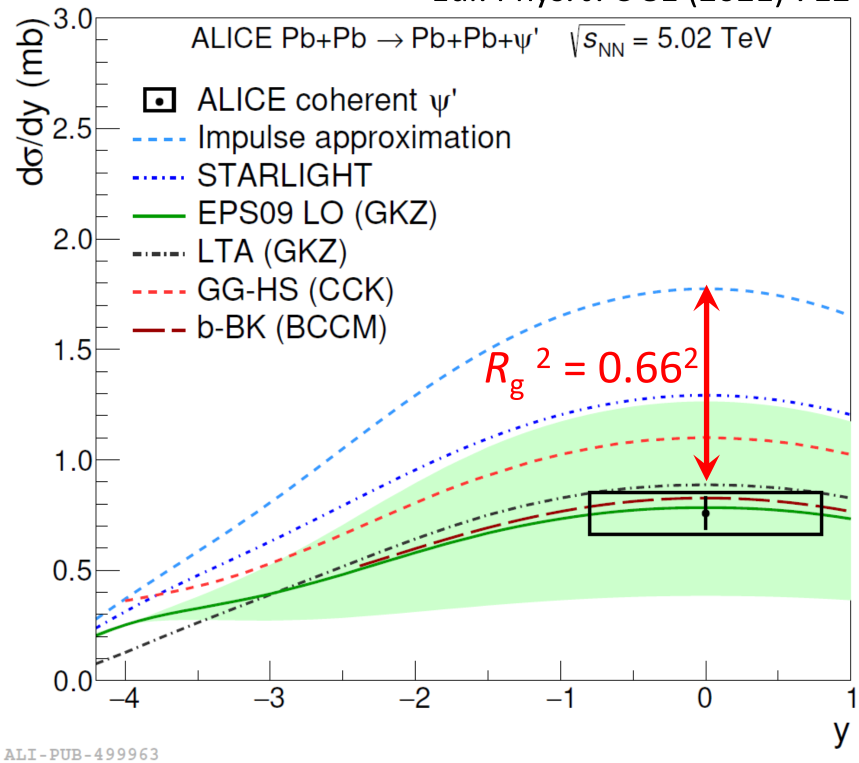

J/ψ in Pb-Pb at $\sqrt{s_{NN}} = 5.02$ TeV

- Central region
  - $J/\psi \rightarrow \mu^+\mu^-$
- $|t|$ dependence is sensitive to spatial gluon distribution
- Bayesian and SVD unfolding used to transform $p_T^2 \rightarrow |t|$
- Transition from UPC to photonuclear cross section

Photon flux

$$\left.\frac{d^2\sigma^{coh}_{J/\psi}}{dy dp_T^2}\right|_{y=0} = 2n_{\gamma Pb}(y=0)\frac{d\sigma_{\gamma Pb}}{d|t|}$$

- Comparison to models:
  - STARlight does not contain explicitly shadowing – do not describe shape nor magnitude
  - LTA contains nuclear shadowing – agrees with data
  - b-BK based on gluon saturation – agrees with data

PLB 817 (2021) 136280

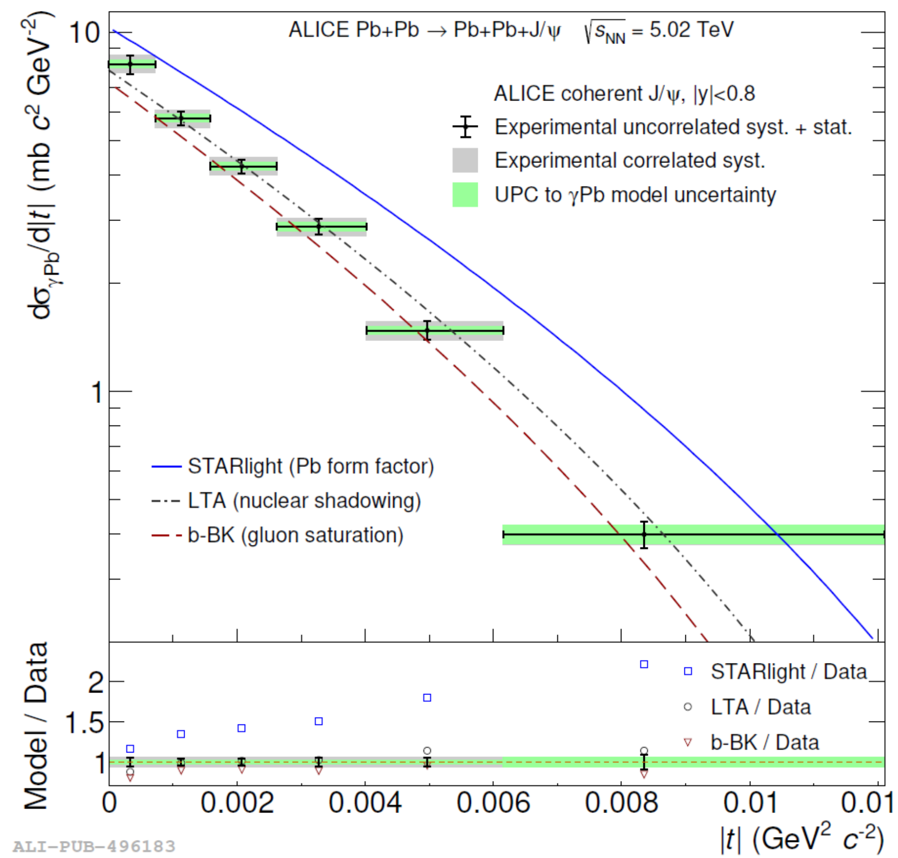

⇒ Reflects effects of QCD dynamics at small $x_B \sim 10^{-3}$

$\gamma\gamma \rightarrow \mu\mu$ in p-Pb at $\sqrt{s_{NN}}$ = 8.16 TeV

- **$\gamma\gamma \rightarrow \mu\mu$ cross section**
- Good agreement of simulation and data
- Comparison with STARlight (LO QED, no FSR) shows slight excess in data
- Important background for other UPC processes
- Constrain theoretical models

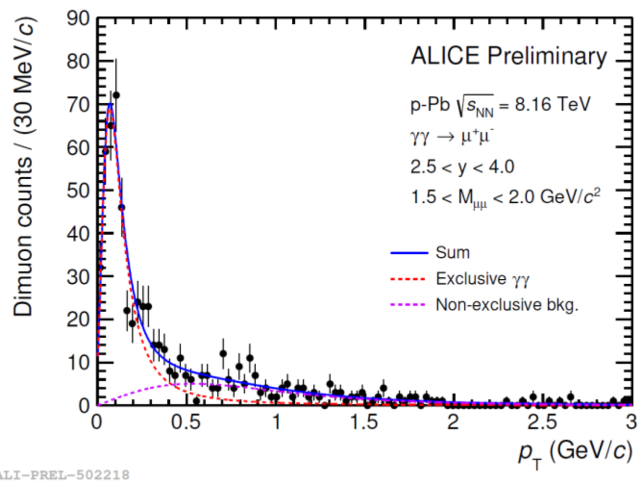

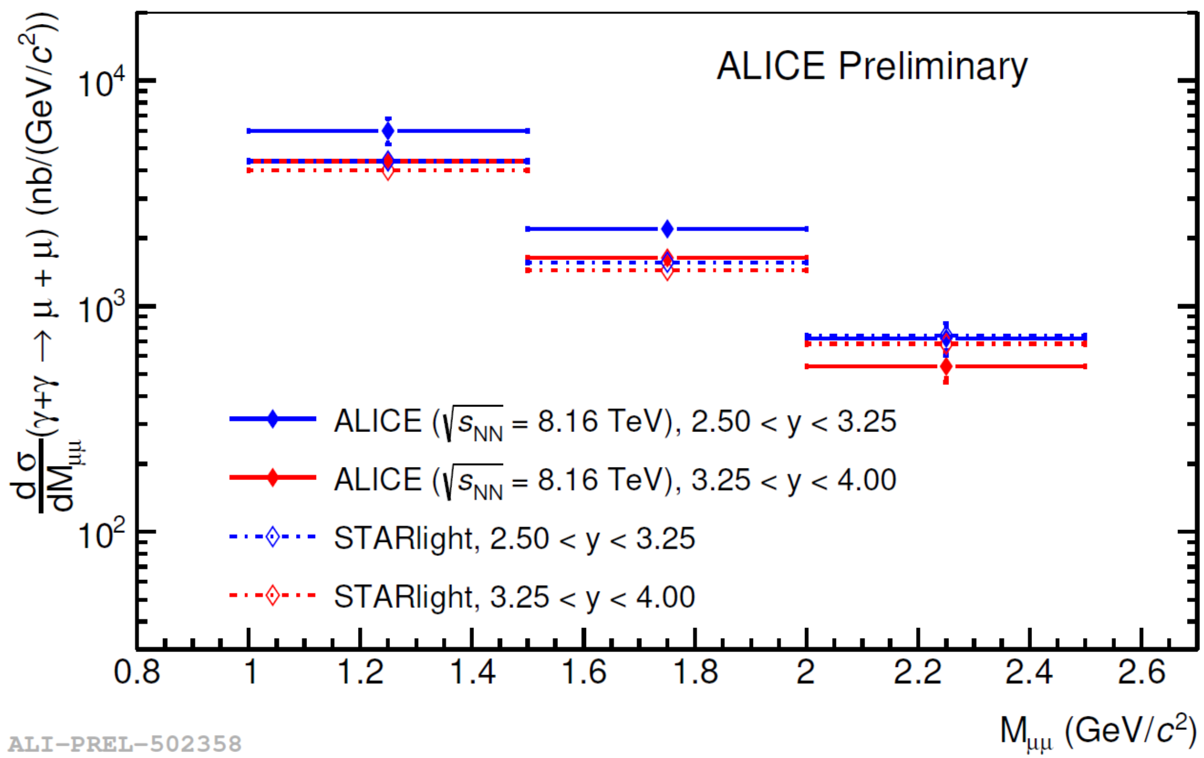

J/ψ in p-Pb at $\sqrt{s_{NN}} = 8.16$ TeV

- Gluon distribution at HERA energies follows power law at low x_B
  $\Rightarrow$ similar trend in $W_{\gamma p}$
- **Exclusive J/ψ cross section** fits well into trend of photo nuclear energy dependence
- A deviation from trend → a change in the evolution of the gluon PDF
  $\Rightarrow$ expected at the onset of saturation

- Power law fit to ALICE data $\sigma \sim W_{\gamma p}{}^{\delta}$ with $\delta = 0.7 \pm 0.04$
  $\Rightarrow$ agreement LHC and HERA
  $\Rightarrow$ agreement ALICE and LHCb
- Models show agreement
  - JMRT NLO: based on DGLAP evolution with dominant NLO contribution
    - valid to $x_B \sim 2 \times 10^{-5}$
  - CCT: Saturation in an energy dependent hot spot model

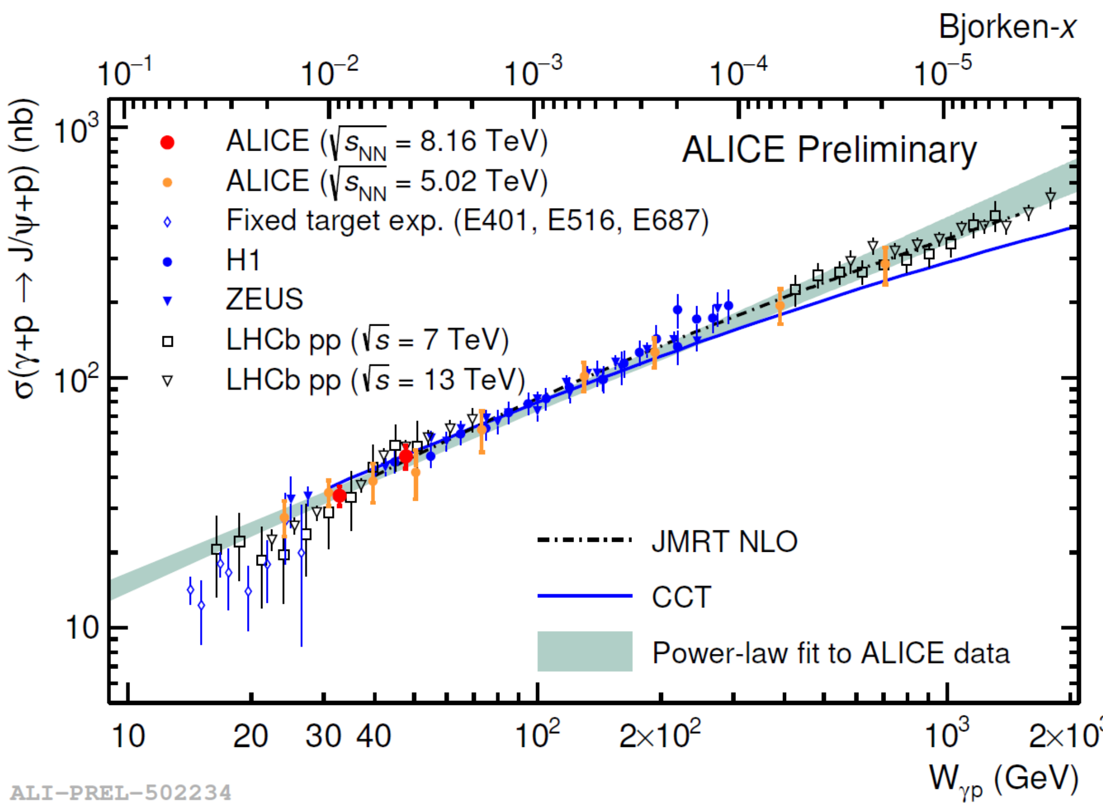

J/ψ in p-Pb at $\sqrt{s_{NN}}$ = 8.16 TeV

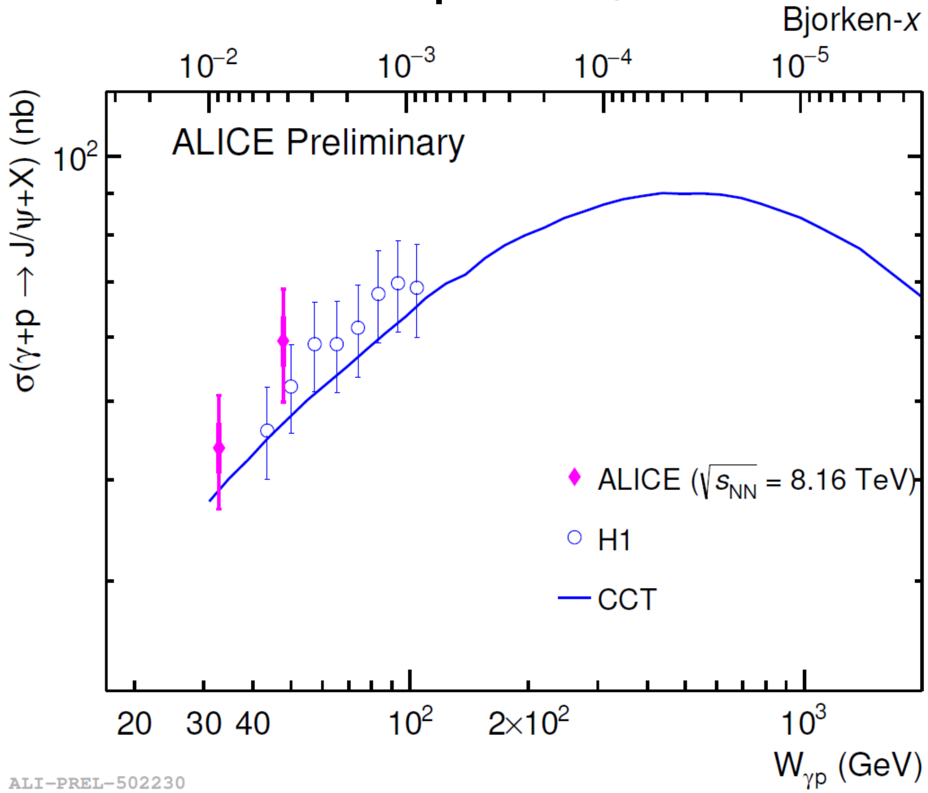

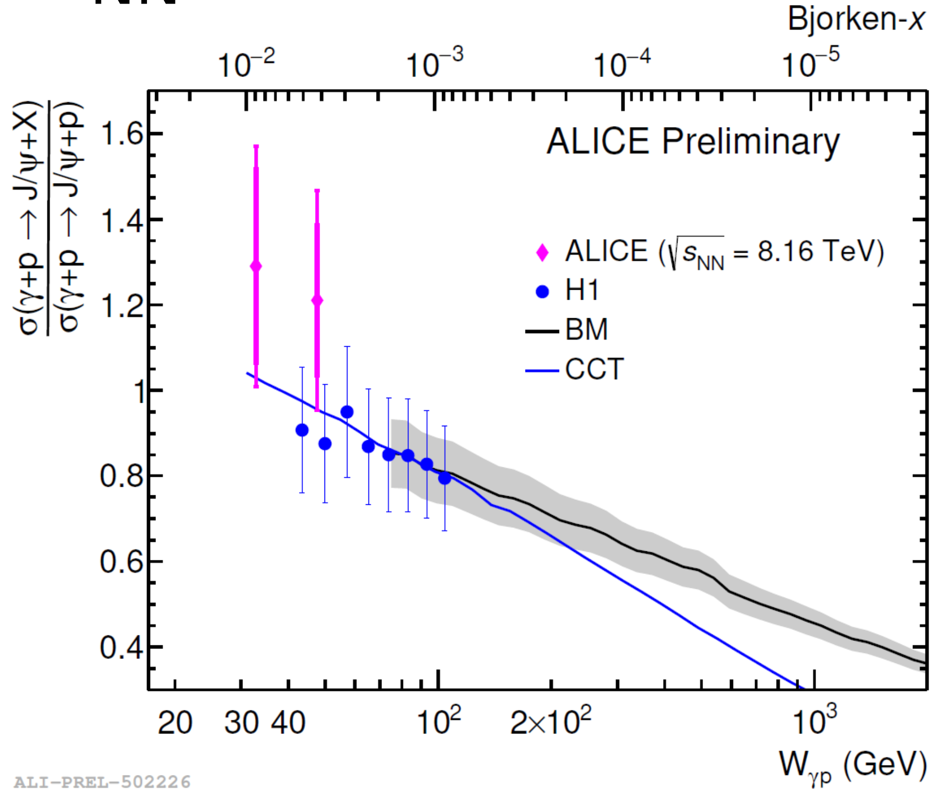

- **First measurement** of the dissociative cross section at the LHC
- Energy dependent **dissociative J/ψ cross section** ($x_B \sim (0.5,2) \times 10^{-2}$)
- Agreement with HERA results
- CCT model with saturation agrees with data
  - Predicted maximum at $W_{\gamma p}$ ~ 500 GeV to be checked in Run 3
- BM: perturbative JIMWLK evolution with parameters constrained to H1 data to be checked in Run 3

LHC and ALICE outline

You are here! (Run 3)

LS2 (between Run 2 and Run 3), LS3 (between Run 3 and Run 4), LS4 (between Run 4 and Run 5)

LHC Schedule	Run 1	Run 2	Run 3	Run 4	Run 5	Run 6
Years	2009 – 2013	2015 – 2018	2022 – 2025	2029 – 2032	2035 – 2038	…
ALICE version	ALICE 1		ALICE 2	ALICE 2.1	ALICE 3	
Collision System	pp, p-Pb, Pb-Pb	pp, p-Pb, Xe-Xe, Pb-Pb	pp, p-O, O-O, p-Pb, Pb-Pb	pp, p-Pb, Pb-Pb	pp, p-A?, A-A	pp, p-A?, A-A

Pb-Pb luminosity $\sim 1\text{-}2 \times 10^{27}$ cm^{-2} s^{-1}

High luminosity for ions $\sim 7 \times 10^{27}$ cm^{-2} s^{-1}

Higher luminosities for ions

HL-LHC
pp luminosity $\sim 4 \times 10^{34}$ cm^{-2} s^{-1}

Period	$L^{Pb\text{-}Pb}$
Run 2	1/nb
Run 3	6/nb
Run 4	7/nb
Run 5*	5.6/nb

* per year

Major upgrade (LS2):
- TPC GEM
- ITS 2
- MFT
- FIT
- O^2 (online-offline)
- All systems readout

Upgrade (LS3):
- ITS 3
- FoCal

Major upgrade (LS4):
Next generation detector

ALICE 2 vs ALICE 3

ALICE in Run 3 + 4 (2022 - 2032 †)

† FoCal upgrade before Run 4

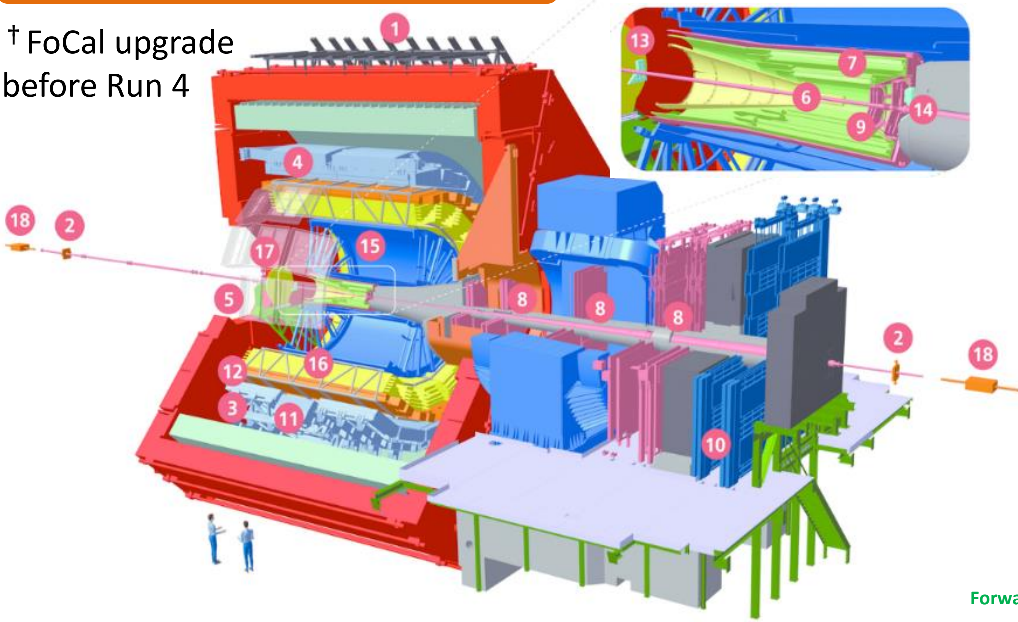

ALICE 3 detector in Run 5 (2035 - 2038)

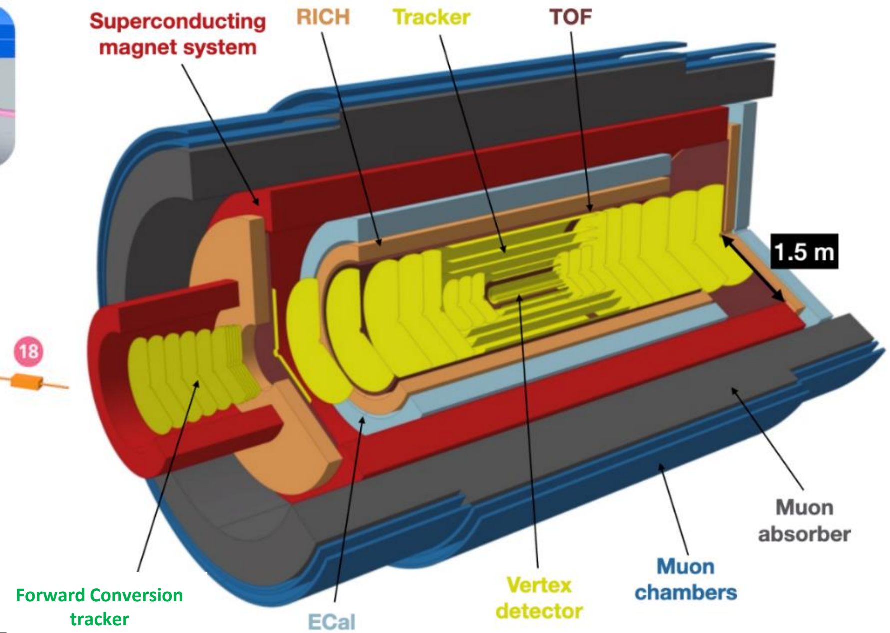

Adamova *et al.*, 1902.01211 (2019); CERN-LHCC-2022-009

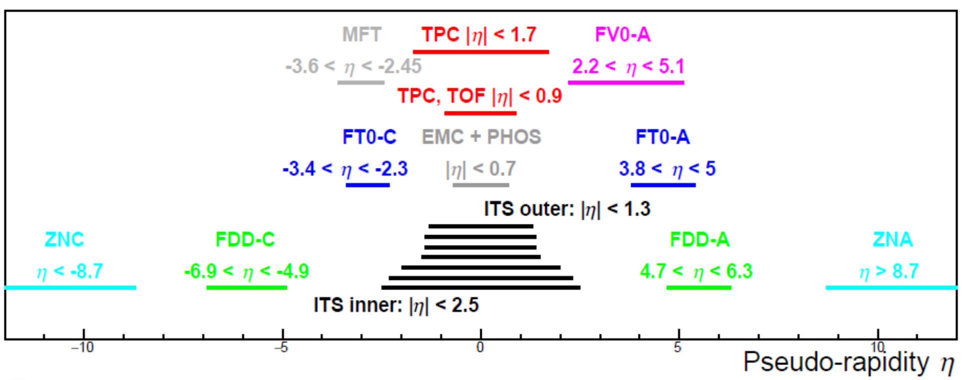

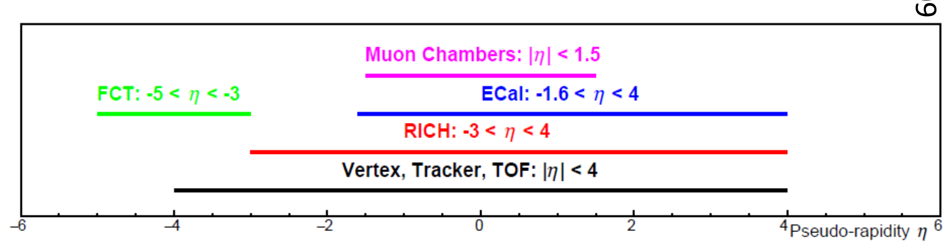

1. **ACORDE** | ALICE Cosmic Rays Detector
2. **AD** | ALICE Diffractive Detector
3. **DCal** | Di-jet Calorimeter
4. **EMCal** | Electromagnetic Calorimeter
5. **HMPID** | High Momentum Particle Identification Detector
6. **ITS-IB** | Inner Tracking System - Inner Barrel
7. **ITS-OB** | Inner Tracking System - Outer Barrel
8. **MCH** | Muon Tracking Chambers
9. **MFT** | Muon Forward Tracker
10. **MID** | Muon Identifier
11. **PHOS / CPV** | Photon Spectrometer
12. **TOF** | Time Of Flight
13. **T0+A** | Tzero + A
14. **T0+C** | Tzero + C
15. **TPC** | Time Projection Chamber
16. **TRD** | Transition Radiation Detector
17. **V0+** | Vzero + Detector
18. **ZDC** | Zero Degree Calorimeter

Run 3 and beyond

- Luminosity increase
- Detector upgrade and continous readout

  $\Rightarrow$ More than 10^4 data with respect to Run 2!

- Precise and new measurements in VM sector
- Light-by-light scattering
- τ anomalous magnetic moment

} + BSM searches

CERN Yellow Rep.Monogr. 7 (2019) 1159

Meson, channel	$\sigma^{\text{Pb-Pb}}$	N^{Tot}	$N^{\lvert\eta\rvert < 0.9}$	$N^{-4 < \eta < -2.5}$
$\rho^0 \to \pi^+ \pi^-$	5.2 b	68×10^9	5.5×10^9	-
$\rho' \to \pi^+ \pi^- \pi^+ \pi^-$	730 mb	9.5×10^9	210×10^6	-
$\phi \to K^+ K^-$	0.22 b	2.9×10^9	82×10^6	-
$J/\psi \to \mu^+ \mu^-$	1.0 mb	14×10^6	1.1×10^6	600×10^3
$\psi(2S) \to \mu^+ \mu^-$	30 μb	400×10^3	35×10^3	19×10^3
$\Upsilon(1S) \to \mu^+ \mu^-$	2.0 μb	26×10^3	2.8×10^3	880

τ pair production

Pair production at LO at LHC for Pb-Pb collisions

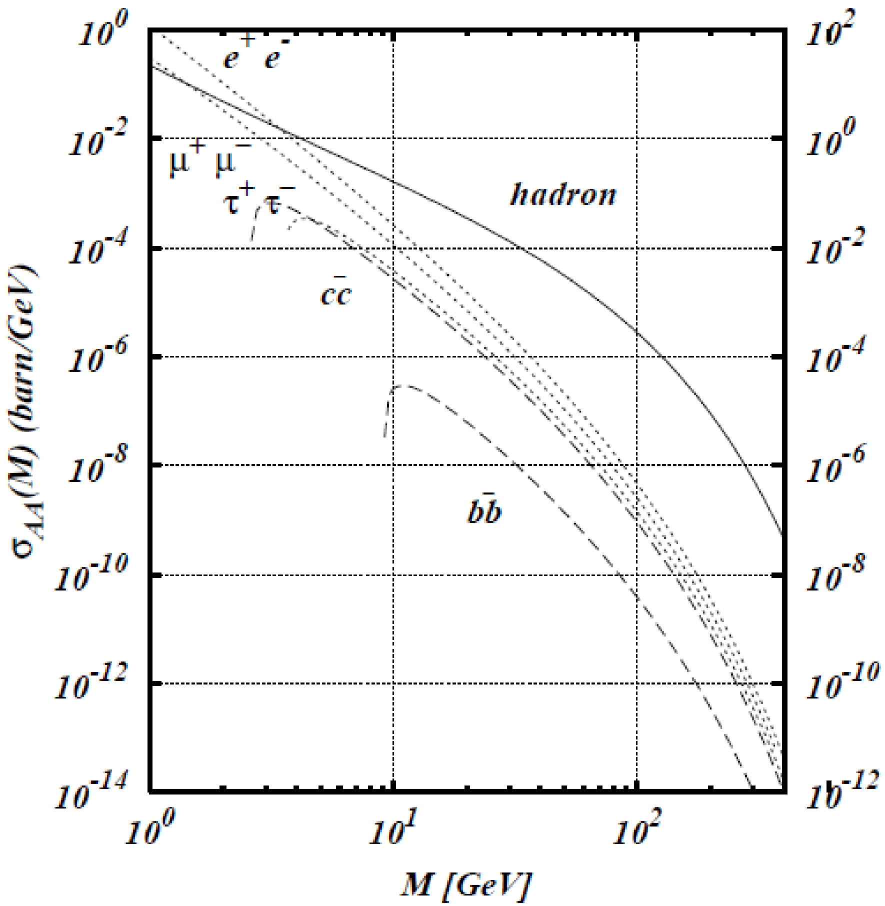

G. Baur at al., hep-ph/0112211 (2001)

- τ pair photoproduction in Pb-Pb UPC → Cross section scales with Z^4
- Suppression by factor $O(\alpha_{em}^2 \approx 5 \times 10^{-5})$
- τ leptons decay quickly and can not be observed directly
  - Lifetime 10^{-13} s
  - Difficult due to at least 1 ν in each τ decay
- Sensitive to anomalous magnetic moment: $a_\ell = (g-2)_\ell/2$

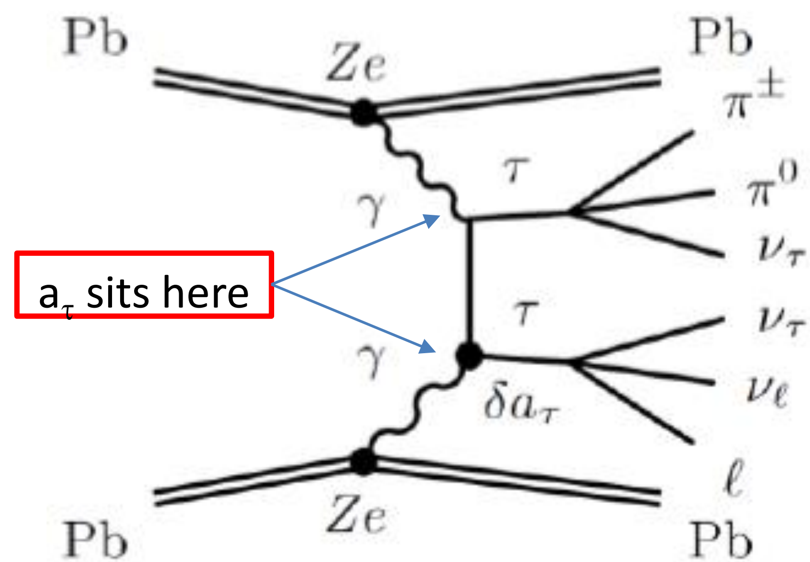

Anomalous magnetic moment

- $a_{\tau(\mu,e)} \neq 0$ because τ lepton (μ, e) is surrounded by virtual particles
- $a_{\tau(\mu,e)} \neq 0$ becomes evident in interaction of τ lepton (μ, e) with external B field
- $a_\ell = (g-2)_\ell/2$
  - g is gyromagnetic moment which relates particle's magnetic moment to its spin $\vec{\mu} = g\frac{q}{2m}\vec{s}$
  - Dirac's equation predicts g = 2
  - Higher order corrections (loops) make g $\neq$ 2
  - Sensitive to particles beyond SM

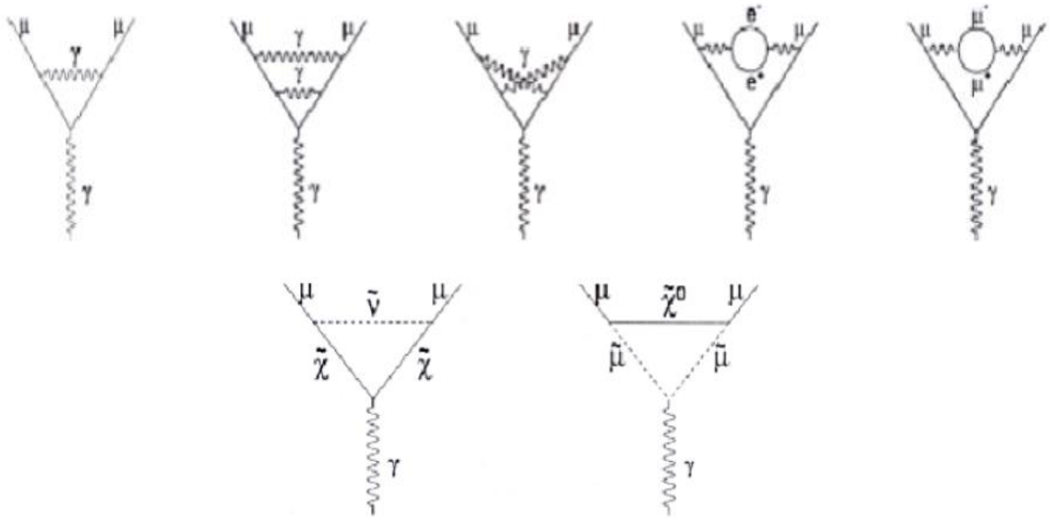

Analysis strategy

- τ decay channels:
  - 1 prong:
    - $BR(\tau^{\pm} \rightarrow \nu_{\tau}\, e^{\pm}\, \nu_l) = 17.8\ \%$
    - $BR(\tau^{\pm} \rightarrow \nu_{\tau}\, \mu^{\pm}\, \nu_l) = 17.4\ \%$
    - $BR(\tau^{\pm} \rightarrow \nu_{\tau}\, h^{\pm}\, n\pi^0) \approx 50\ \%$ ($h = \pi, K$)
  - 3 prongs:
    - $BR\ (\tau^{\pm} \rightarrow \nu_{\tau}\, 3\pi^{\pm}\, n\pi^0) \approx 15\ \%$
- Event topology:
  - 1+1 tracks $\sim$ 70 %
    - e, μ, π, K tracks
  - 1+3 tracks $\sim$ 25 %
    - e, μ, π, K tracks + 3 charged π
- Reject dilepton continuum production
- Use displaced vertex for 3 prong τ decay

p_T and acoplanarity spectra

L. Beresford, J. Liu, PRD 102 (2020) 113008

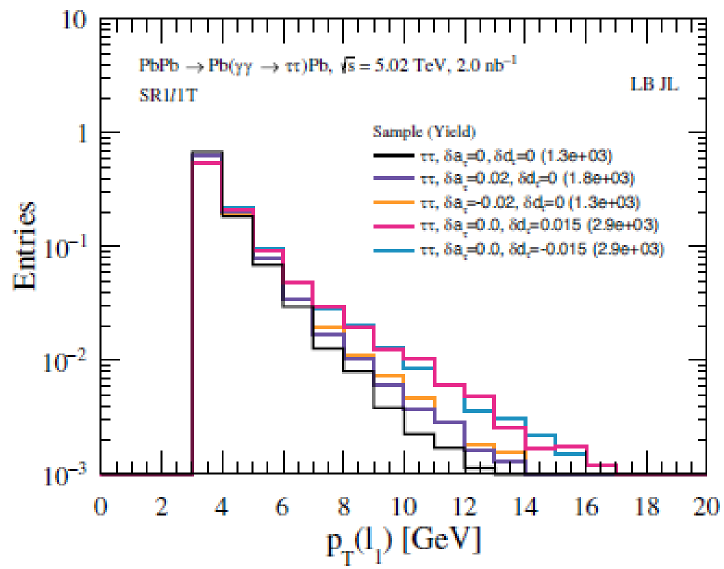

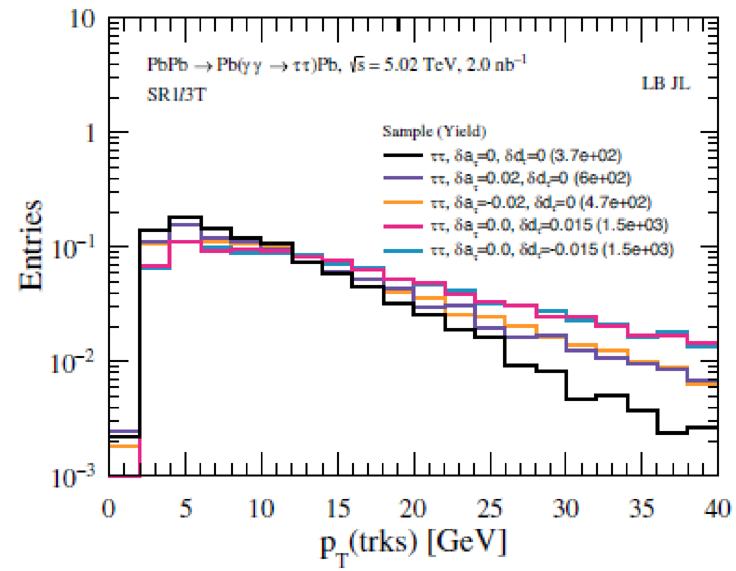

- p_T differential spectra give better a_τ sensitivity
- Expectations for different a_τ
- Acoplanarity shows large background reduction power

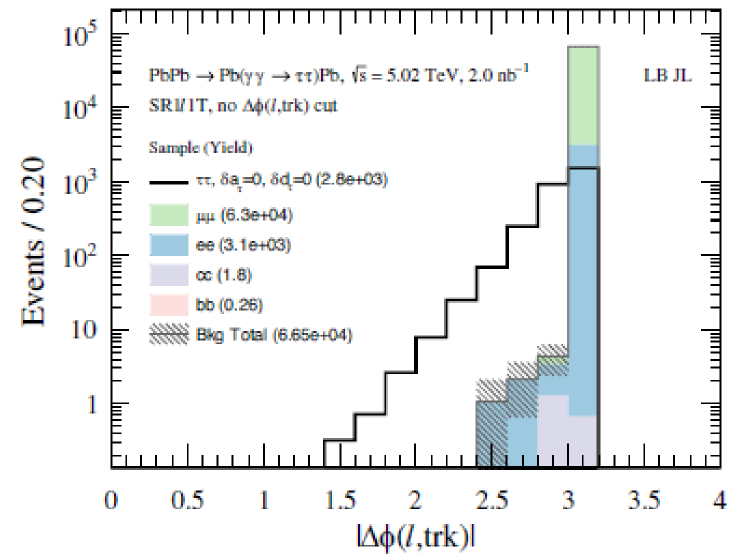

ALICE in Run 3 expectations

Burmasov et al., 2203.00990 (2022)

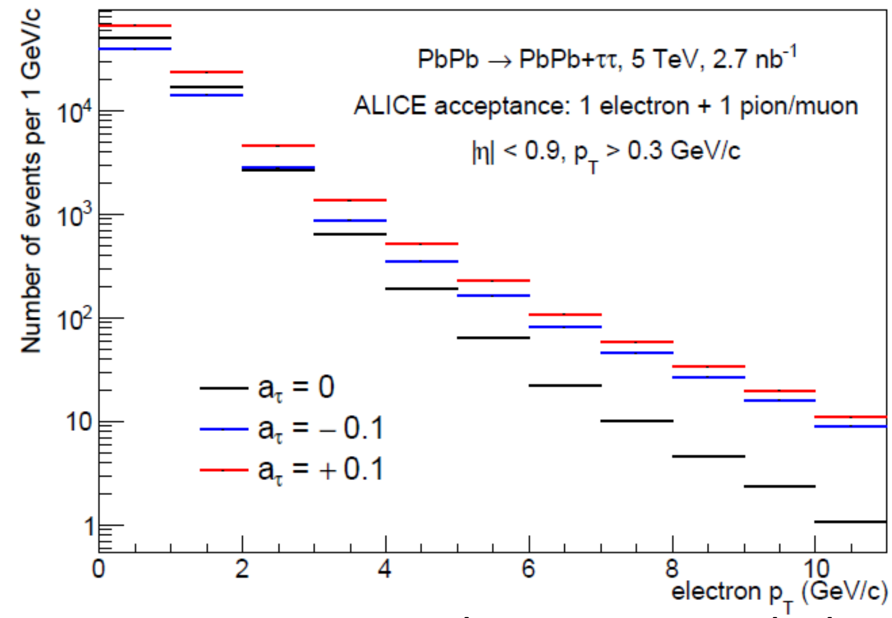

Burmasov et al., 2203.00990 (2022)

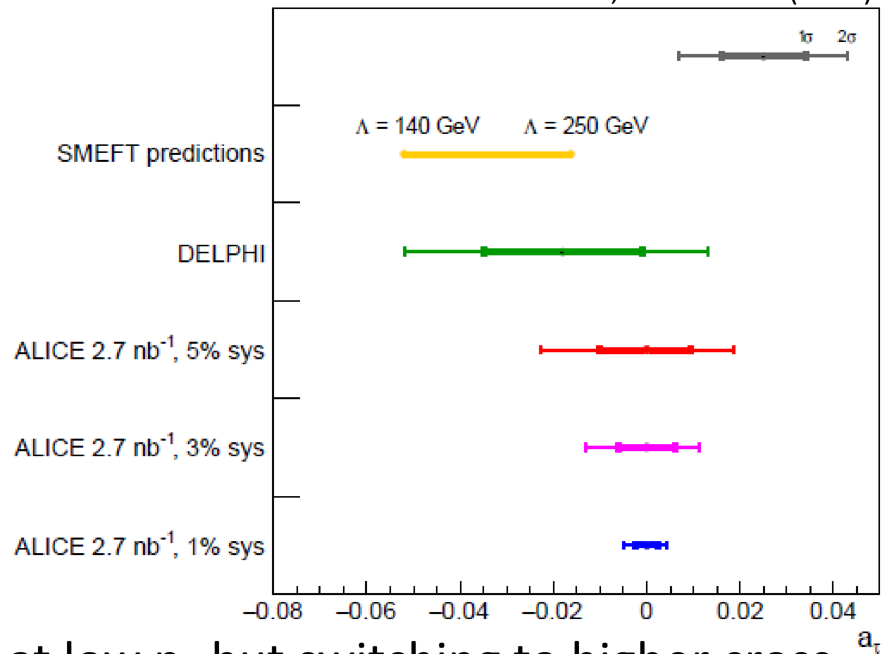

- Cross sections with a_τ = -0.1 are below SM at low p_T but switching to higher cross sections starting from p_T^e > 3 GeV/c → p_T differential measurements provide better sensitivity
- At least x2 improvements on a_τ limits with Pb-Pb data to be collected in the first year (2023 ???) with current ALICE (2)
- ALICE 3 will provide much more data
  - Finner binning
  - Lower p_T accesibility
  - Larger η range
  - Better PID (not only electrons will be used)

Light-by-light scattering

- Pure quantum effect
- Contributes to electron/muon anomalous magnetic moment (g-2)
- Challenging process: $O(\alpha_{em}^4 \approx 3 \times 10^{-9})$
- Quarks, leptons or W bosons can be exchanged in the loop in the lowest order
- Higher order corrections allow also for mesons exchange: η, $\eta'(958)$, $\eta_c(1S)$, $\eta_c(2S)$, $\chi_{c0}(1P)$, …
- There is a place for Beyond Standard Model physics: SUSY particles, spin-even resonances (ALPs), magnetic monopoles, …
- Cross section is calculated by several groups

PRC93 (2016) 044907

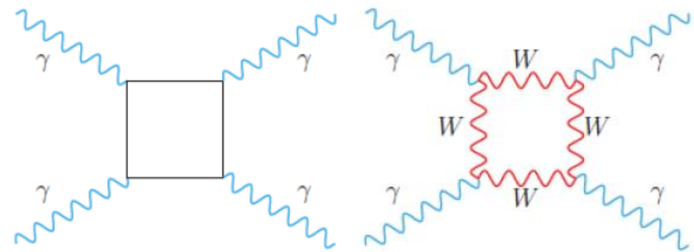

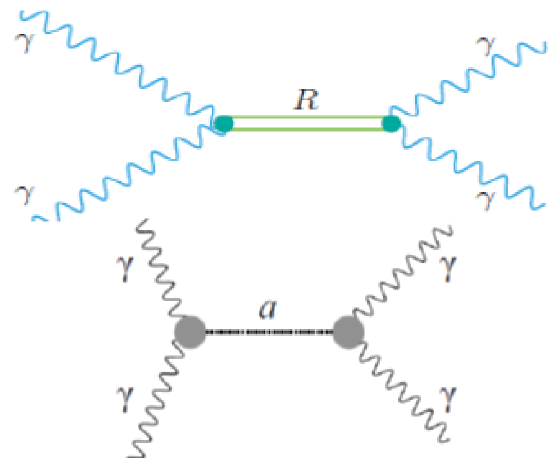

PRD 99, 093013 (2019)

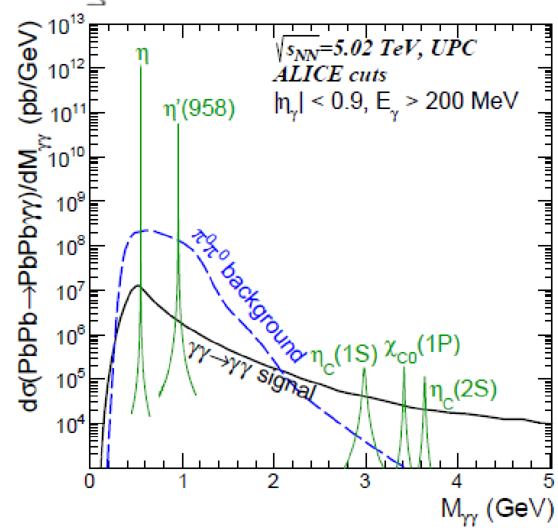

PRD 99, 093013 (2019)

Feasibility studies for ALICE 2 and 3

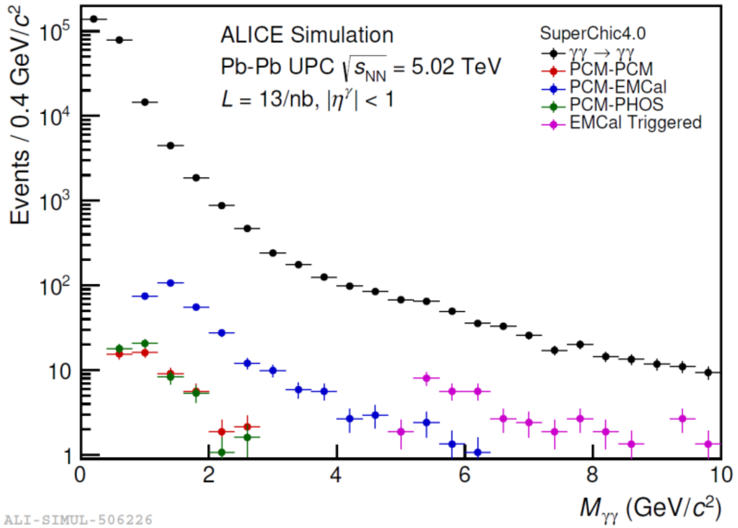

$$A_S = \left| \frac{|\vec{p}_T(1)| - |\vec{p}_T(2)|}{|\vec{p}_T(1)| + |\vec{p}_T(2)|} \right|$$

Background reduction with A_S variable

ALICE3 LOI: CERN-LHCC-2022-009 / LHCC-I-038

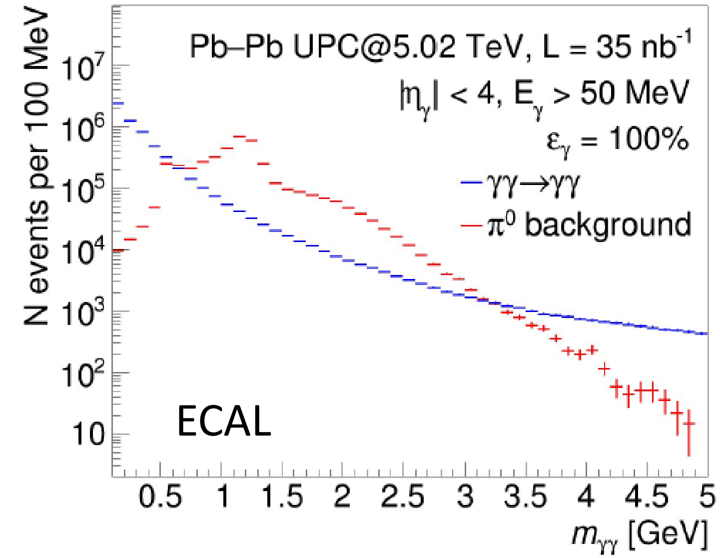

Considered topologies in Run 3 and 4

Both γ's reconstructed with Photon Conversion Method (PCM) from e^+e^- pairs

- $p_T^{\gamma,\ PCM} > 0.1$ GeV/c

One γ via PCM, other in EMCal acceptance

- $p_T^{\gamma,\ EMCal} > 0.5$ GeV/c
- $p_T^{\gamma,\ PCM} > 0.1$ GeV/c

One γ via PCM, other in PHOS acceptance

- $p_T^{\gamma,\ PHOS} > 0.3$ GeV/c
- $p_T^{\gamma,\ PCM} > 0.1$ GeV/c

Both γ's in EMCal acceptance, one triggered

- $p_T^{\gamma,\ EMCal} > 0.5$ GeV/c
- $p_T^{\gamma,\ EMCal\ triggerd} > 2.5$ GeV/c

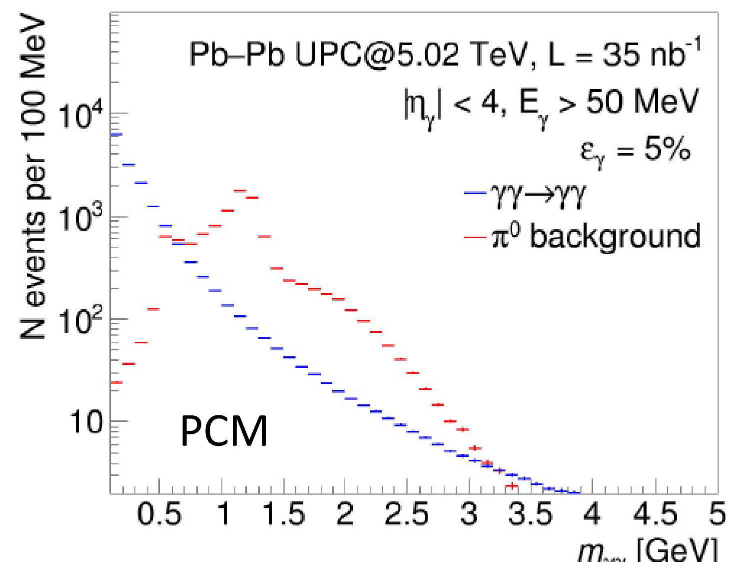

Expected upper limits for ALP production

- Poissonian limits for ALPs in UPCs at $\sqrt{s_{NN}}$ = 5.5 TeV (Based on PRL 118, 171801 (2017))
- Signal: ALPs from STARlight; $\Gamma(a \to \gamma\gamma) = 1/64\pi\, m_a^3/\Lambda^2$
- Background: L-by-L, $\pi^0\pi^0$, fake electrons and bremsstrahlung
- Asymmetry requirement $A_S < 0.02$

- ALICE 3 is designed to measure very low particle p_T
- ALiCE 3 can provide complementary result in low mass region 50 MeV/c^2 < $M_{\gamma\gamma}$ < 5 GeV/c^2

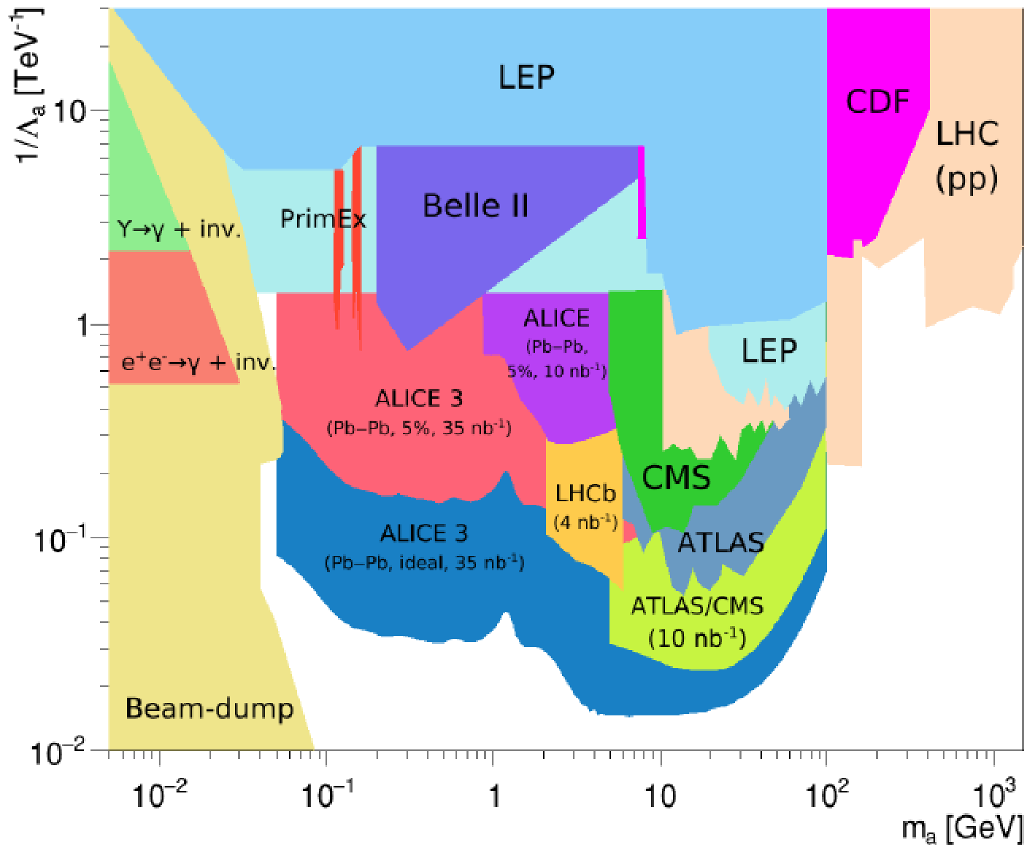

Summary

- Light VM photoproduction signals large shadowing effects
  - No model describes all the breakup classes (0nXn is the most difficult)
- Resonance-like structure at $M^{\pi\pi}$ ~ 1.7 GeV/c^2
- Nuclear gluon structure probed with J/ψ at $x_B \sim 10^{-3}$
  - Nuclear gluon shadowing factor $R_g \sim 0.65$
  - Models with shadowing or saturation describe data the best
  - No model describe all the rapidity points
  - |t|dependence is sensitive to spatial gluon distribution
- Proton gluon structure probed at $x_B \sim 10^{-2}$
  - Agreement of exclusive and dissociative J/ψ photoproduction with saturation models
  - Agreement with previous results
  - First measurement of the dissociative cross section at the LHC
- Analyses of data coming from Run 3 and beyond will provide new exciting results

Backup

Coverage

- V0A: $2.8 < \eta < 5.1$, $z = 3.4$ m
- V0C: $-3.7 < \eta < -1.7$, $z = -0.9$ m
- ADA: $4.7 < \eta < 6.3$, $z = 16.9$ m
- ADC: $-6.9 < \eta < -4.9$, $z = -19.5$ m
- ZDC: $z = \pm 112.5$ m, $|\eta| > 8.8$

Triggers

- Central barrel trigger
  - ρ^0 in Pb-Pb — $L = 485 \pm 24$ mb^{-1}
    - Veto in AD and V0
    - SPD topology $\Delta\varphi > 153°$
  - ρ^0 in Xe-Xe — $L = 279.5 \pm 29.9$ mb^{-1}
    - Veto in V0
    - SPD and TOF signal
  - J/ψ, ψ' in Pb-Pb — $L^{\text{Central}} = 233$ μb^{-1}
    - Veto in AD, V0
    - SPD and TOF topology $\Delta\varphi > 153°$
    - Signal in central barrel ITS, TPC, TOF

- Forward trigger
  - J/ψ, ψ' in Pb-Pb — $L^{\text{Forward}} = 754 \pm 38$ μb^{-1}
    - Veto in SPD, AD, V0
    - Signal in muon spectrometer
  - J/ψ in p-Pb — $L = 7.62 \pm 0.14$ nb^{-1}
    - Veto in AD, V0
    - Signal in muon spectrometer

VM photoproduction publications

- Coherent photoproduction of ρ^0 vector mesons in ultra-peripheral Pb-Pb collisions at $\sqrt{s_{NN}}$ = 5.02 TeV, JHEP 06 (2020) 035.
- First measurement of coherent ρ^0 photoproduction in ultra-peripheral Xe-Xe collisions at $\sqrt{s_{NN}}$ = 5.44 TeV, Phys. Lett. B 820 (2021) 136481.
- Coherent J/ψ photoproduction at forward rapidity in ultra-peripheral Pb-Pb collisions at $\sqrt{s_{NN}}$ = 5.02 TeV, Phys.Lett. B798 (2019) 134926.
- Coherent J/ψ and ψ′ photoproduction at midrapidity in ultra-peripheral Pb-Pb collisions at $\sqrt{s_{NN}}$ = 5.02 TeV, Eur. Phys. J. C 81 (2021) 712.
- First measurement of the |t|-dependence of coherent J/ψ photonuclear production, PLB 817 (2021) 136280.
- Energy dependence of exclusive J/ψ photoproduction off protons in ultra-peripheral p-Pb collisions at $\sqrt{s_{NN}}$ = 5.02 TeV, Eur. Phys. J. C (2019) 79: 402.

ρ^0 – ZDC energy

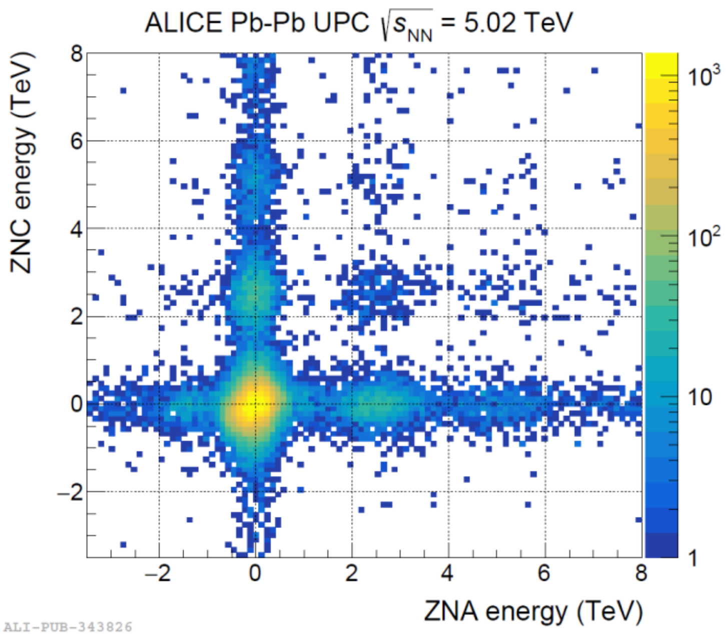

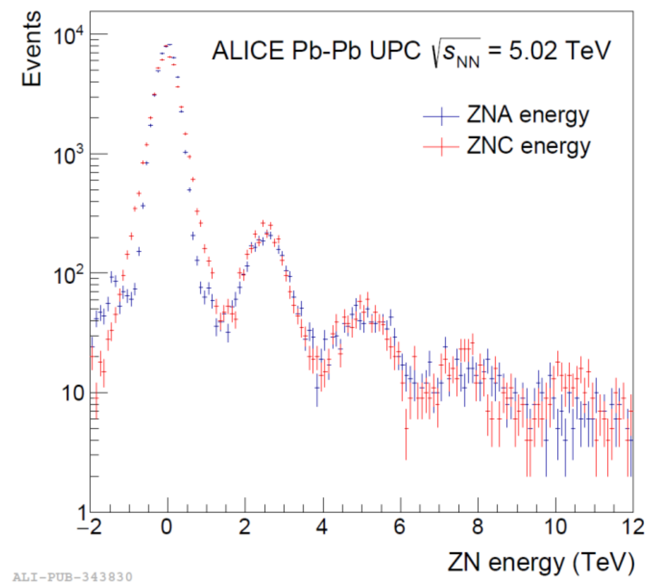

ρ^0 in Xe-Xe

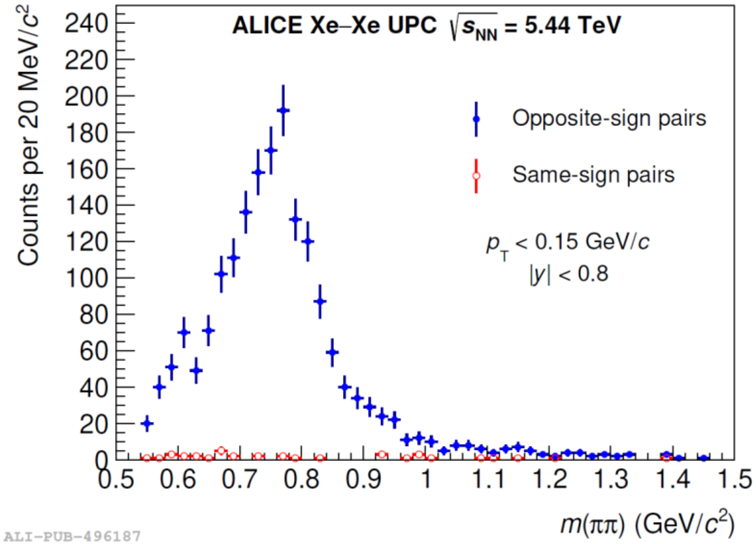
ALICE Xe–Xe UPC $\sqrt{s_{NN}}$ = 5.44 TeV
Opposite-sign pairs
Same-sign pairs
p_T < 0.15 GeV/c
$|y|$ < 0.8
Counts per 20 MeV/c^2
$m(\pi\pi)$ (GeV/c^2)
ALI-PUB-496187

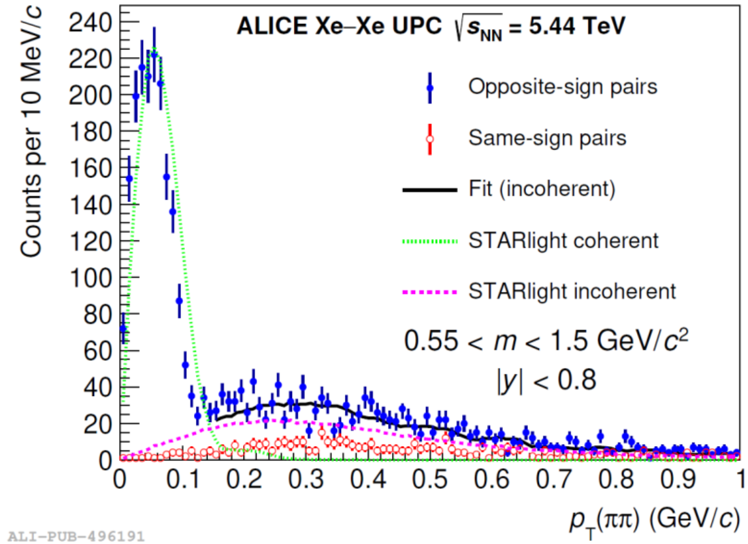
ALICE Xe–Xe UPC $\sqrt{s_{NN}}$ = 5.44 TeV
Opposite-sign pairs
Same-sign pairs
Fit (incoherent)
STARlight coherent
STARlight incoherent
0.55 < m < 1.5 GeV/c^2
$|y|$ < 0.8
Counts per 10 MeV/c
$p_T(\pi\pi)$ (GeV/c)
ALI-PUB-496191

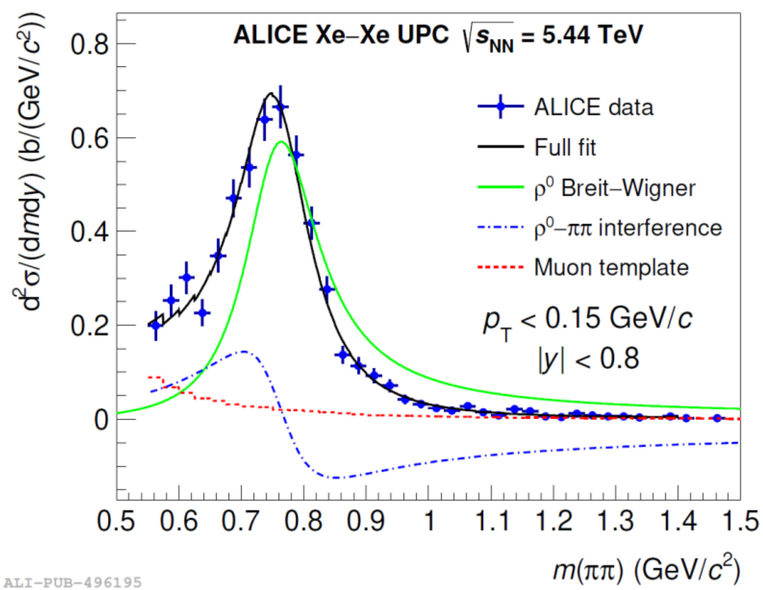
ALICE Xe–Xe UPC $\sqrt{s_{NN}}$ = 5.44 TeV
ALICE data
Full fit
ρ^0 Breit–Wigner
ρ^0–$\pi\pi$ interference
Muon template
p_T < 0.15 GeV/c
$|y|$ < 0.8
$d^2\sigma/(dmdy)$ (b/(GeV/c^2))
$m(\pi\pi)$ (GeV/c^2)
ALI-PUB-496195

J/ψ in Pb-Pb – forward

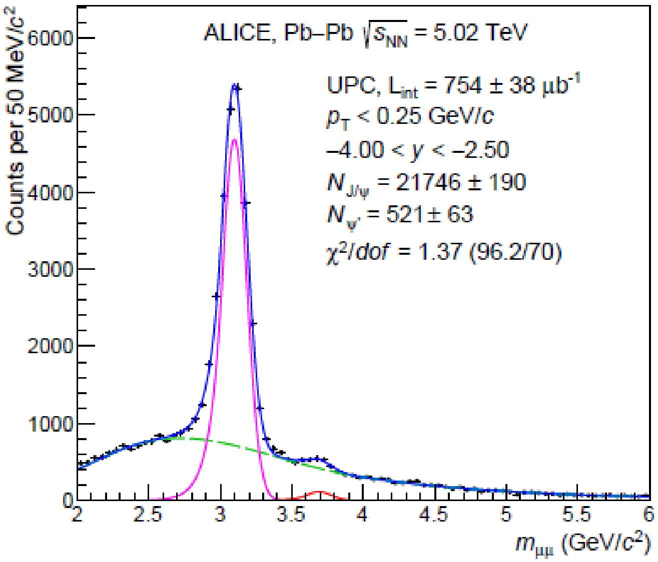

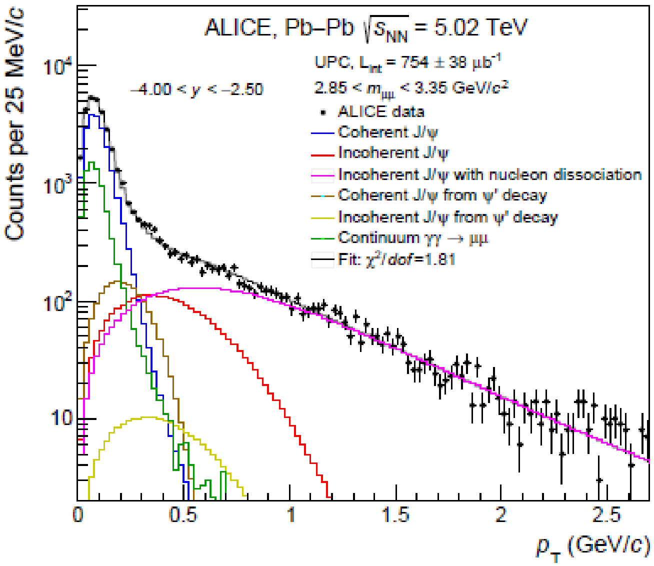

J/ψ in Pb-Pb – central barrel

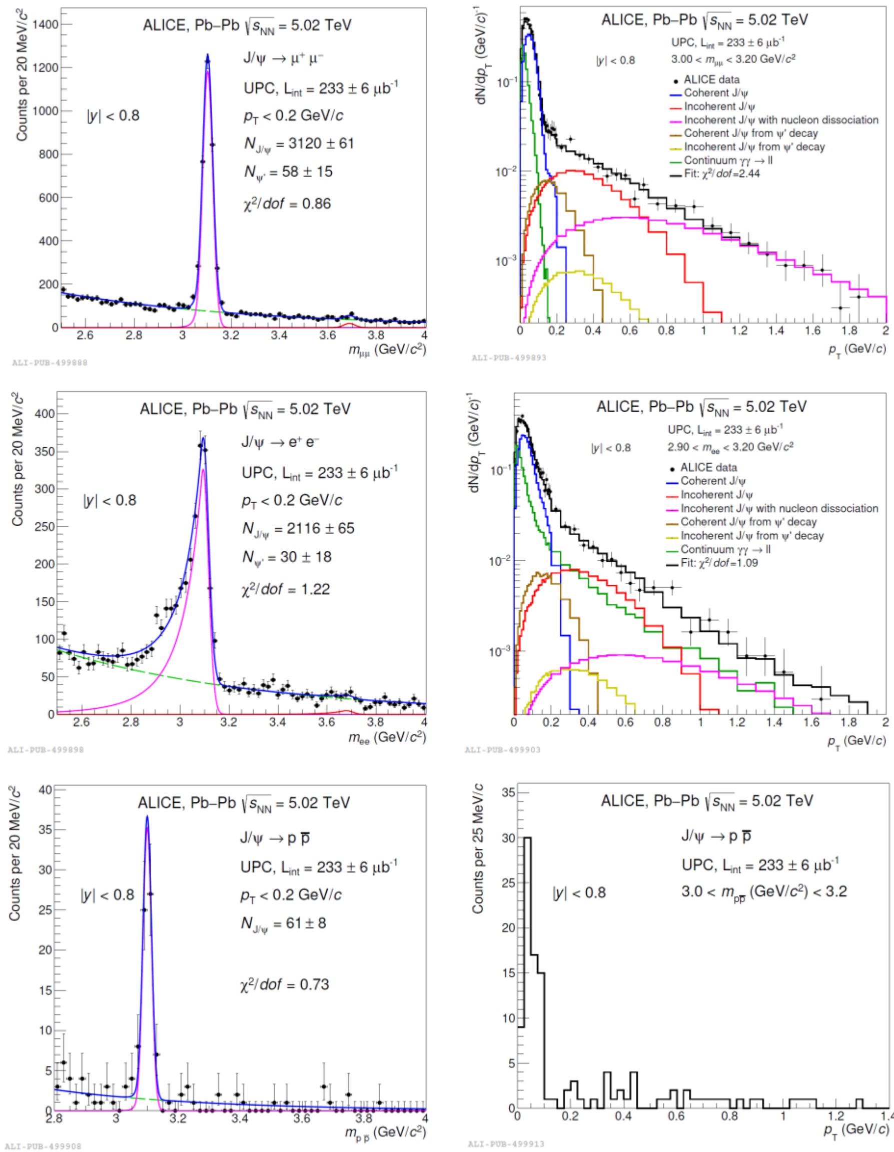

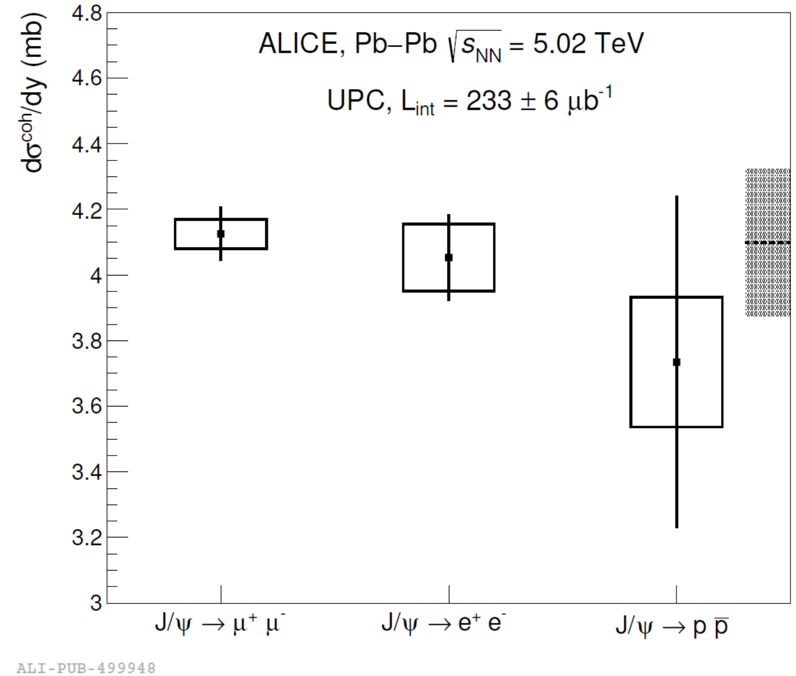

ψ' in Pb-Pb – central barrel

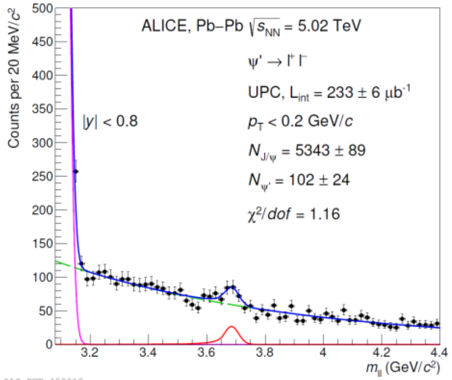

ALI-PUB-499918

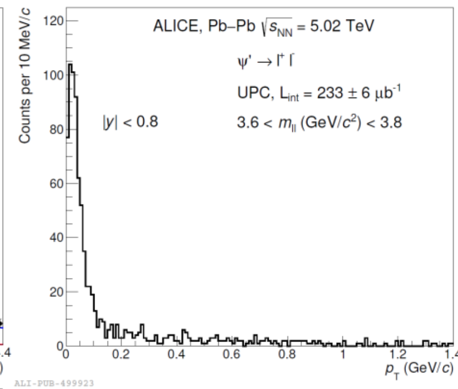

ALI-PUB-499923

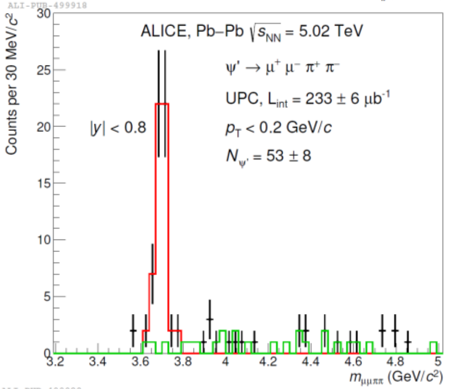

ALI-PUB-499928

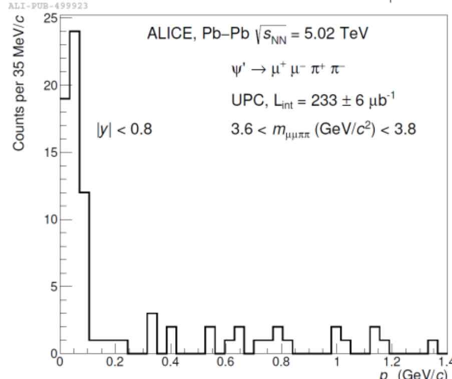

ALI-PUB-499933

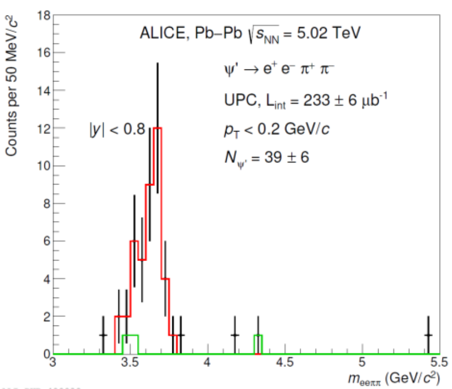

ALI-PUB-499938

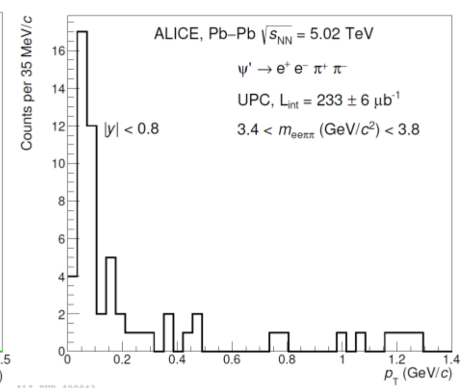

ALI-PUB-499943

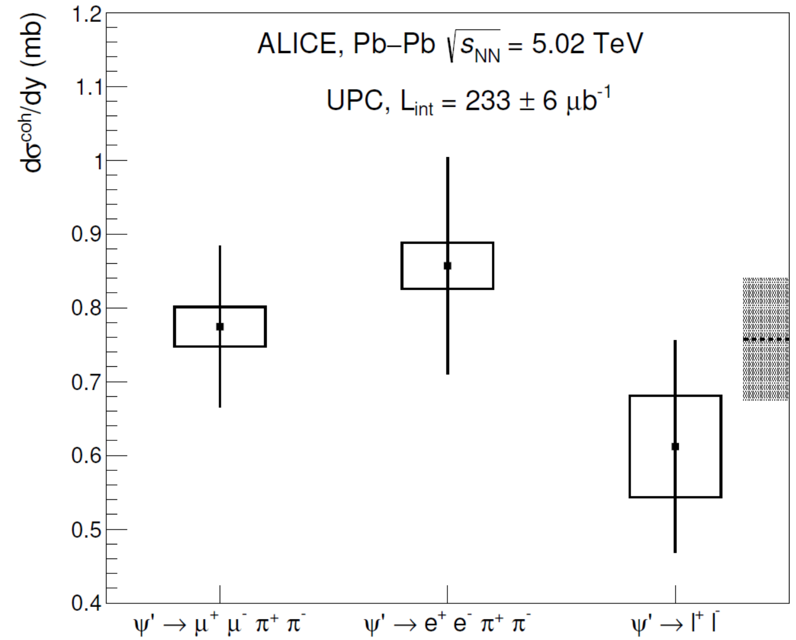

ALI-PUB-499953

Exclusive J/ψ in p-Pb

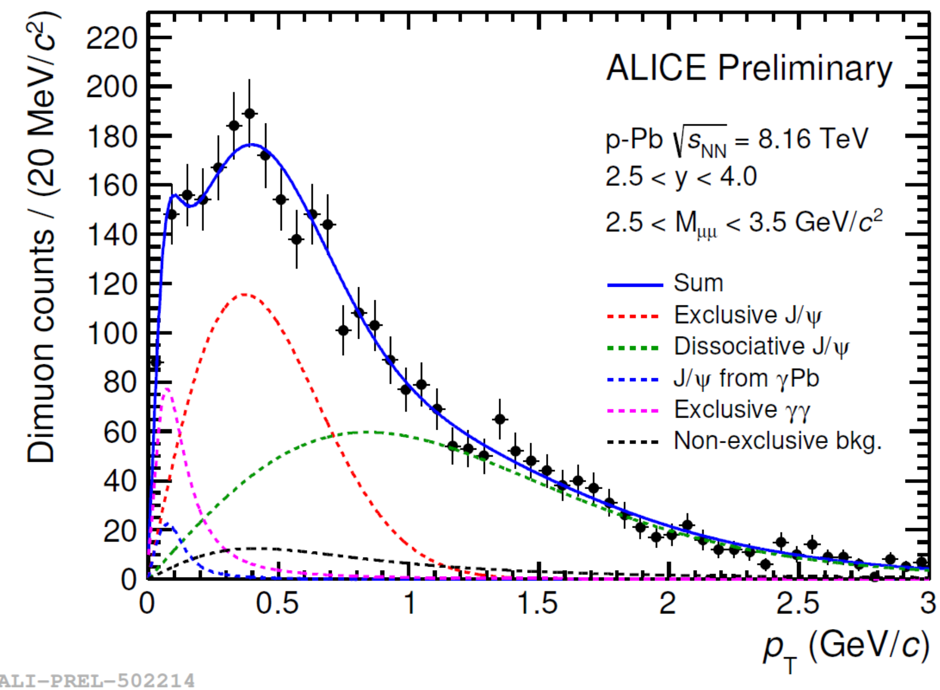

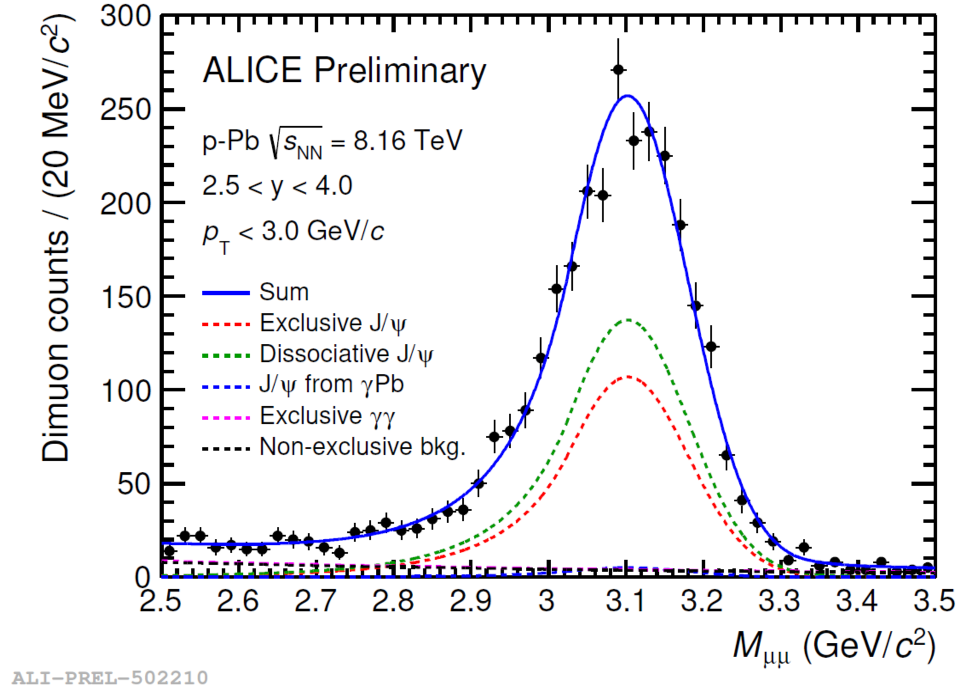

Cross section parameterization

$$\frac{d\sigma}{dm\,dy} = |A \cdot BW_\rho + B|^2 + M,$$

$$BW_\rho = \frac{\sqrt{m \cdot m_{\rho^0} \cdot \Gamma(m)}}{m^2 - m_{\rho^0}^2 + i m_{\rho^0} \cdot \Gamma(m)}$$

$$\Gamma(m) = \Gamma(m_{\rho^0}) \cdot \frac{m_{\rho^0}}{m} \cdot \left(\frac{m^2 - 4m_\pi^2}{m_{\rho^0}^2 - m_\pi^2}\right)^{3/2}$$

Soding formula

- A – normalization
- B – non resonsnt amplitude
- M – other background
- BW_ρ – Breit-Wigner function
- Γ(m) – mass dependent width
- $m_{\rho 0}$ – pole mass
- m_π - pion mass

ρ_3(1690) with angular momrentum J = 3

$$\frac{dN_{\pi\pi}}{dm} = P_1 \cdot \exp(-P_2 \cdot (m - 1.2\,\mathrm{GeV}/c^2)) + P_3 + P_4 \cdot \exp(-(m - M_x)^2/\Gamma_x^2)$$

VM cross section

$$\frac{d\sigma^{coh}_{VM}}{dy} = \frac{N^{coh}_{VM}}{\varepsilon_{VM} \times \varepsilon^{pileup}_{veto} \times \varepsilon^{EMD}_{veto} \times BR \times \mathscr{L}_{int} \times \Delta y}$$

$$N^{coh}_{J/\psi} = \frac{N_{yield}}{1 + f_I + f_D}$$

$$N^{coh}_{\psi'} = \frac{N_{yield}}{1 + f_I}.$$

- N_{yield} – J/ψ or ψ' raw yield,
- ε_{VM} - reconstruction efficiency
- f_I – incoherent contamination fraction
- f_D – feed down contamination fraction
- L_{int} – integrated luminosity
- Δy – rapidity interval
- BR – branching ratio of the Decay
- $\varepsilon^{pileup}{}_{veto}$ – pileup veto efficiency
- $\varepsilon^{EMD}{}_{veto}$ – electromagnetic dissociation veto efficiency

Shadowing and saturation

- Shadowing – the experimental fact that the nuclear structure functions are suppressed compared to the superposition of those of their constituent nucleons.
  - N. Armesto, “Nuclear shadowing”, J. Phys. G 32 (2006) R367–R394.
- Saturation – a dynamic equilibrium between gluon radiation and recombination.
  - J. L. Albacete and C. Marquet, “Gluon saturation and initial conditions for relativistic heavy ion collisions”, Prog. Part. Nucl. Phys. 76 (2014) 1–42.

Models

- **Black disk limit:**
  - Frankfurt, Strikman, Zhalov, *Phys. Lett.* B537 (2002) 51–61.
  - total cross section of the interaction is equal to $2\pi R_A^2$.
- **STARlight:**
  - Klein, Nystrand, Seger, Gorbunov, Butterworth, Comput. Phys. Commun. 212 (2017) 258–268; Klein and Nystrand, Phys. Rev. C 60 (1999) 014903.
  - Based on a phenomenological description of the exclusive production of VM off nucleons, the optical theorem, and a Glauber-like eikonal formalism, does not take into account the elastic part of the elementary VM–nucleon cross section.
  - Includes multiple scattering, **no gluon shadowing**.
- **GKZ (Guzey, Kryshen and Zhalov):**
  - Guzey, Kryshen, Zhalov, Phys. Rev. C93 (2016) 055206; Frankfurt, Guzey, Strikman, Zhalov, Phys. Lett. B752 (2016) 51–58.
  - Based on a modified **vector dominance model**, in which the hadronic fluctuations of the photon interact with the nucleons in the nucleus according to the Gribov-Glauber model of **nuclear shadowing**
- **GMMNS (Goncalves, Machado, Morerira, Navarra and dos Santos):**
  - Gonçalves, Machado, Moreira, Navarra, dos Santos, Phys. Rev. D96 (2017) 094027; Iancu, Itakura, Munier, Phys. Lett. B590 (2004) 199–208,
  - Based on the Iancu-Itakura-Munier (IIM) implementation of **gluon saturation** within the **colour dipole model** coupled to a boosted-Gaussian description of the wave function of the vector meson.
- **CCKT (Cepila, Contreras, Krelina and Tapia):**
  - Cepila, Contreras, Tapia Takaki, Phys. Lett. B766 (2017) 186–191; Cepila, Contreras, Krelina, Tapia Takaki, Nucl. Phys. B934 (2018) 330–340; N. Armesto, Eur. Phys. J. C26 (2002) 35–43
  - Based on the **colour dipole model** with the structure of the nucleon in the transverse plane described by so-called **hot spots**, regions of high gluonic density, whose number increases with increasing energy. The nuclear effects are implemented along the ideas of the Glauber model. Version without hot spots (named *nuclear*) and including them.
  - Indicates **gluon saturation**.

Models

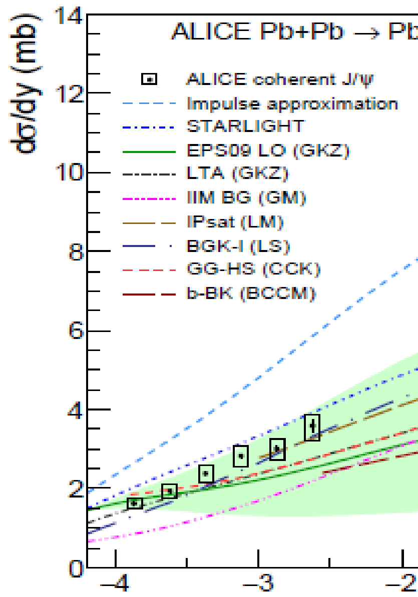

- **Impulse approximation:**
  - Exclusive photoproduction off protons, neglects all nuclear effects but coherence.
  - Based on STARlight.
- **EPS09 LO:**
  - GKZ model with parameterization of **nuclear shadowing** data.
  - Eskola, Paukkunen, Salgado, JHEP 04 (2009) 065.
- **LTA:**
  - GKZ model based on Leading Twist Approximation of **nuclear shadowing**.
  - Frankfurt, Guzey, Strikman, Phys. Rept. 512 (2012) 255–393.
- **IIM BG, IPsat, BGK-I:**
  - **Color dipole** approach coupled to the Color Glass Condensate (CGC) formalism with different assumptions on the dipole-proton scattering amplitudę.
  - Gonçalves, Moreira, Navarra, Phys. Rev. C 90 (2014) 015203; dos Santos, Machado, J. Phys. G 42 no. 10, (2015) 105001. (saturation)
  - Lappi, Mäntysaari, Phys. Rev. C 83 (2011) 065202; Lappi, Mäntysaari, Phys. Rev. C 87 (2013) 032201. (saturation)
  - A. Łuszczak, Schäfer, Phys. Rev. C 99 no. 4, (2019) 044905. (shadowing)
- **GG-HS**:
  - CCK **color dipol model** with **hot spots** nucleon structure with Glauber-Gribov formalism
  - Cepila, Contreras, Krelina, Phys. Rev. C 97 no. 2, (2018) 024901; Cepila, Contreras, Tapia Takaki, Phys. Lett. B766 (2017) 186–191.
- **b-BK:**
  - Bendova, Cepila, Contreras, Matas (BCCM) model based on the **color dipole** approach coupled to the impact-parameter dependent Balitsky-Kovchegov equation with initial conditions based on the Woods-Saxon shape of the Pb nucleus.
  - Bendova, Cepila, Contreras, Matas, Physics Letters B 817 (2021) 136306.

Models

- noon:
  - Broz, Contreras, Tapia Takaki, “A generator of forward neutrons for ultra-peripheral collisions: nOOn”, Comput. Phys. Commun. (2020) 107181.
- JMRT NLO:
  - next-to-leading-order calculations
  - Jones, Martin, Ryskin, Teubner, J. Phys. G 44 no. 3, (2017) 03LT01; JHEP 11 (2013) 085.
- BM:
  - Perturbative JIMWLK evolution based on HERA data
  - Mantysaari, Schenke, Phys. Rev. D 98 no. 3, (2018) 034013

Systematic uncertainty

ρ^0 in Pb-Pb

Source	Uncertainty
Variations to the fit procedure	0.4–5.9 %
Ross-Stodolsky fit model	+3.5%
Track selection	±1.5%
Track matching	±4.0%
Acceptance and efficiency	±1.0%
Muon background ($\gamma\gamma \rightarrow \mu^+\mu^-$)	±0.3%
Incoherent contribution	±0.5%
Trigger efficiency of SPD chips	±1.0%
Pile-up	±3.8%
Luminosity	±5.0%
Total	$^{+(8.5-10.3)}_{-(7.8-9.7)}$ %

ρ^0 in Xe-Xe

Source	Uncertainty
Variations to the fit procedure	±2.5%
Ross–Stodolsky fit model	+3.5%
Acceptance and efficiency	±0.5%
Track selection	±3.0%
Track ITS–TPC matching	±4.0%
SPD trigger-to-track matching	±2.0%
TOF trigger efficiencies	±2.8%
Vertex selection	±1.5%
Incoherent contribution	±2.0%
Pile-up	±1.0%
Muon background ($\gamma\gamma \rightarrow \mu^+\mu^-$)	$^{+(0.5)}_{-(0.2)}$ %
Electromagnetic dissociation	±0.2%
Luminosity	±10.7%
Total	$^{+(13.3)}_{-(12.8)}$ %

Source	No forward-neutron selection	0n0n	0nXn	XnXn
Signal either in ZNA or in ZNC	$^{-1.0}_{+1.1}$	±0.1	$^{-6.6}_{+7.3}$	$^{+0.6}_{-0.7}$
Signal in both ZNA and ZNC	$^{-0.3}_{+0.4}$	±0.7	$^{+0.3}_{-0.4}$	$^{-8.9}_{+10.6}$

Class	Measured fraction	$\mathbf{n_O^O n}$ prediction
0n0n	$(90.46 \pm 0.70 \pm 0.17 \mp 0.68)\%$	92.4%
0nXn+Xn0n	$(8.48 \pm 0.66 \mp 0.13 \pm 0.64)\%$	6.9%
XnXn	$(1.07 \pm 0.25 \mp 0.04 \pm 0.07)\%$	0.7%

Systematic uncertainty

- J/ψ forward

Source	Value
Lumi. normalization	$\pm 5.0\%$
Branching ratio	$\pm 0.6\%$
SPD, V0 and AD veto	from -3.6% to -6.0%
MC rapidity shape	from $\pm 0.1\%$ to $\pm 0.8\%$
Tracking	$\pm 3.0\%$
Trigger	from $\pm 5.2\%$ to $\pm 6.2\%$
Matching	$\pm 1.0\%$
Signal extraction	$\pm 2.0\%$
f_{D} fraction	$\pm 0.7\%$
$\gamma\gamma$ yield	$\pm 1.2\%$
p_{T} shape for coherent J/ψ	$\pm 0.1\%$
b_{pd} parameter	$\pm 0.1\%$
Total	from $^{+8.3}_{-9.2}\%$ to $^{+8.9}_{-10.3}\%$

- J/ψ central

	$\mathrm{J}/\psi \to \mu^+\mu^-$	$\mathrm{J}/\psi \to e^+e^-$	$\mathrm{J}/\psi \to \mathrm{p}\overline{\mathrm{p}}$
Signal Extraction	0.5	2.4	0.7
Incoherent contamination	0.8	0.5	0.8
Branching ratio	0.5	0.5	1.4
TOF matching	–	–	5.0
ITS-TPC matching	2.8	2.8	2.8
AD and V0 veto	3.0	3.0	3.0
SPD trigger efficiency	1.0	1.0	1.0
TOF trigger efficiency	0.7	0.7	0.7
Luminosity	2.7	2.7	2.7
EMD correction	2.0	2.0	2.0
Feed down	0.6	0.6	0.6
Channel uncorrelated	1.1	2.5	5.3
Channel correlated	5.5	5.5	5.5

Systematic uncertainty

- ψ’ central

	$\psi' \to \mu^+\mu^-\pi^+\pi^-$	$\psi' \to e^+e^-\pi^+\pi^-$	$\psi' \to l^+l^-$
Signal Extraction	1.0	2.0	10.0
Incoherent contamination	1.4	1.8	1.8
Branching ratio	1.5	1.5	4.8
ITS-TPC matching pions	2.8	2.8	–
ITS-TPC matching leptons	2.8	2.8	2.8
AD and V0 veto	10.0	10.0	10.0
SPD trigger efficiency	1.0	1.0	1.0
TOF trigger efficiency	0.7	0.7	0.7
Luminosity	2.7	2.7	2.7
EMD correction	2.0	2.0	2.0
Channel uncorrelated	3.5	5.8	11.2
Channel correlated	11.0	11.0	11.0

J/ψ central t dep.

Source	Uncertainty (%)
Signal extraction	(0.7,2.2)
f_D	(0.1,0.5)
f_I	(1.1,2.3)
p_T^2 migration unfolding	(0.6,2.3)
Luminosity	2.7
V0 and AD veto	3
EM dissociation	2
ITS-TPC tracking	2.8
SPD and TOF efficiency	1.3
Branching ratio	0.5
Variations in interference strength	(0.3,1.2)
Value of the photon flux at $y = 0$	2
$p_T^2 \to \|t\|$ unfolding	(0.1,5.7)

Upgrade - Inner Tracking System (ITS) v2

- Newly designed beam pipe with a smaller outer radius of 19 mm
- 7 layers of Monolithic Active Pixel Sensors (MAPS)
  - Area ~10 m^2
  - Smaller material budget: ~ 0.35% X_0 per layer for layers 0-2, ~ 0.8% for layers 3-6 (was ~ 1.1% for ITS1)
  - Power consumption < 40 mW/cm^2

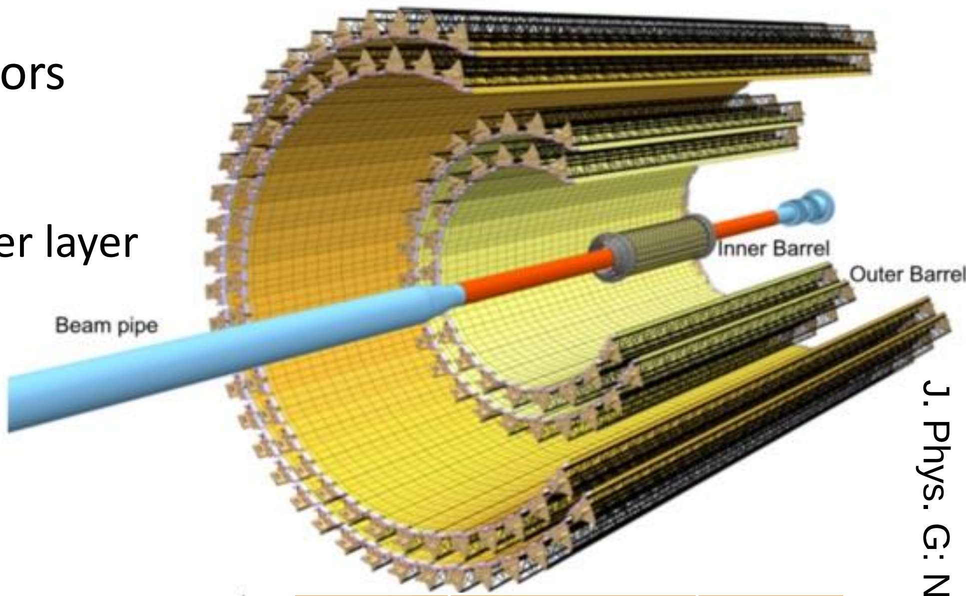

J. Phys. G: Nucl. Part. Phys. **41** (2014) 087002

- Faster readout rate
  - up to ~50 kHz in Pb-Pb (1 kHz in ITS1)
  - ~500 kHz in pp
- Improved tracking and resolution
  - Spatial resolution ~5 μm
  - Impact parameter resolution:
    - 3 × better in the transverse plane
    - 5 × better along the beam axis
  - Momentum resolution ~ 4% at 2 GeV/*c*
  - p_T down to very low values
- More precise vertexing in higher rates with resolution better than 100 μm

Layer	R_{min} [mm]	η
0	22.4	± 2.5
1	30.1	± 2.3
2	37.8	± 2.0
3	194.4	± 1.5
4	243.9	± 1.4
5	342.3	± 1.4
6	391.8	± 1.3

ITS installation

Inner barrel

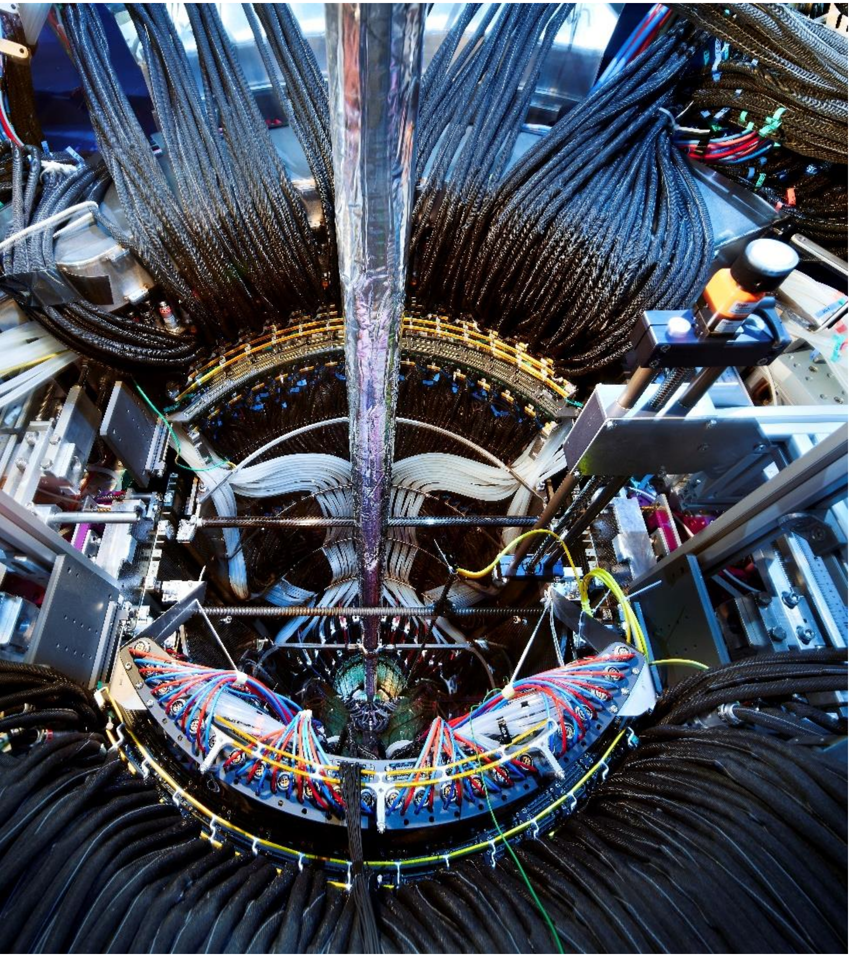

Outer barrel

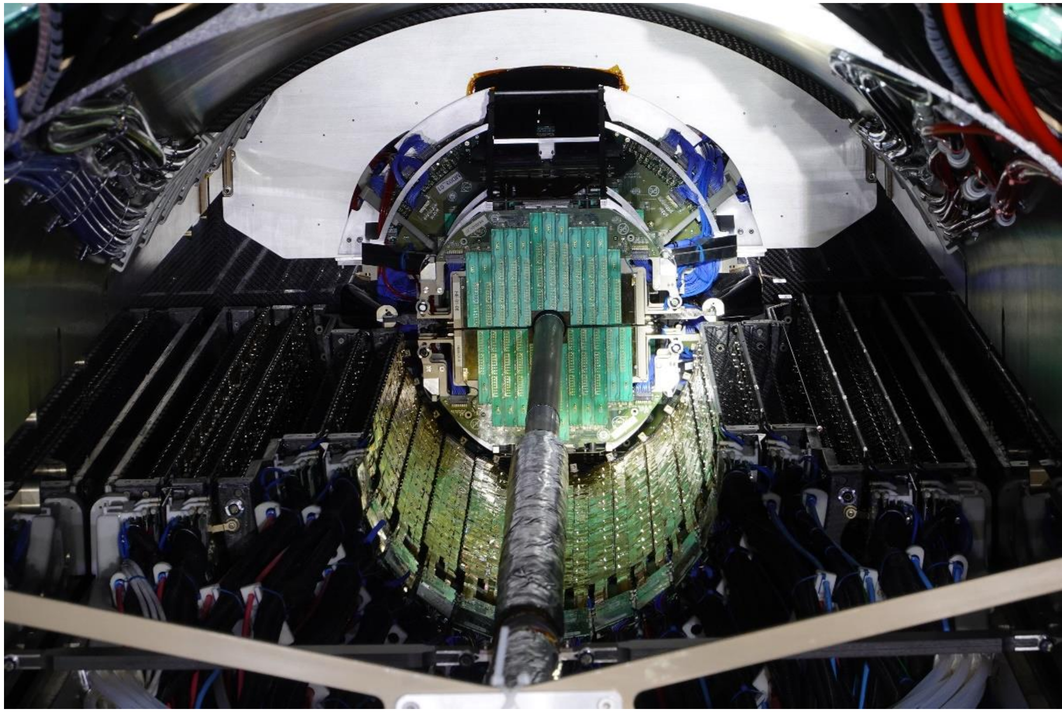

Time Projection Chamber (TPC)

- Gas Electron Multiplier (GEM) technology readout
- Continuous readout
- Factor 100 increase of data collection rate
- Tracking and PID remains the same
- 1 stack in IROC, 3 stacks in OROC
- Ion Back Flow < 1% at gain = 2000
- Local energy resolution $\sigma_E/E < 12\%$ for ^{55}Fe

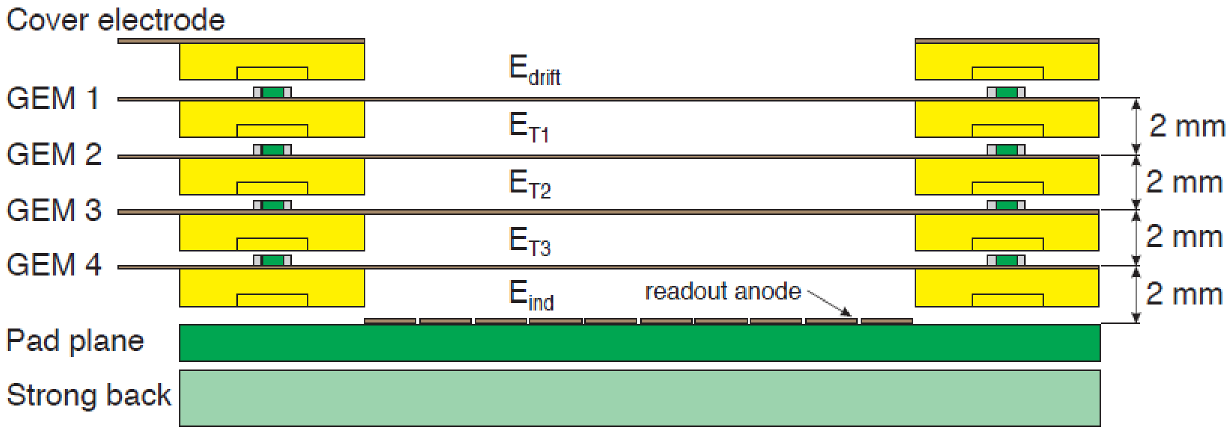

CERN-LHCC-2013-020 (2014),
CERN-LHCC-2015-002 (2015)

Muon Forward Tracker (MFT)

- Two half-cones
- Five detection disks
- -460 mm $< z <$ -768 mm
- $-3.6 < \eta < -2.45$
- Technology similar to ITS 2
- Material budget 0.6% X_0 per disk
- Spatial resolution ~5 μm

⇒ Access for prompt J/ψ or ψ(2S) production and nuclear modification factors R_{AA} down to zero p_T.

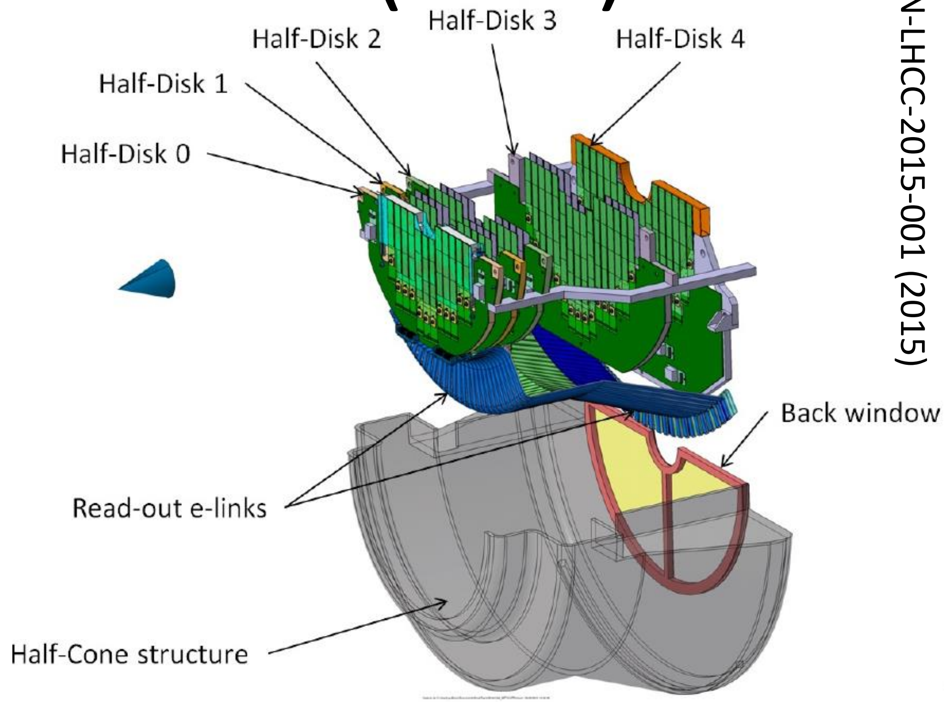

CERN-LHCC-2015-001 (2015)

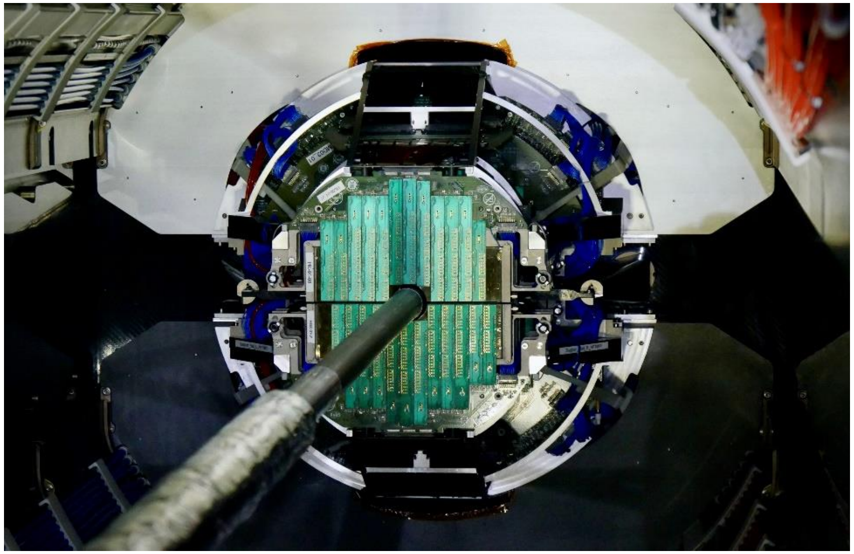

Fast Interaction Trigger (FIT)

- Interaction trigger
- Online luminometer
- Beam quality
  - Beam – gas events
  - Background conditions
- Vertex position indicator
- Forward multiplicity counter
  - Centrality
  - Event plane

FT0:

- Quartz Cherenkov radiators
- Time resolution $\sigma_t \approx 13$ ps
- $z^{T0A} = 3.3$ m and $z^{T0C} = -84$ cm
- 96 and 112 modules

FV0:

- Large scintillator disk
- 8 cm < R < 144 cm
- 48 sectors
- Trigger with latency < 425 ns

FDD:

- Two arrays of scintillator pads
- 8 channels each side
- $z^{DDA} = 16.9$ m and $z^{DDC} = -19.5$ m

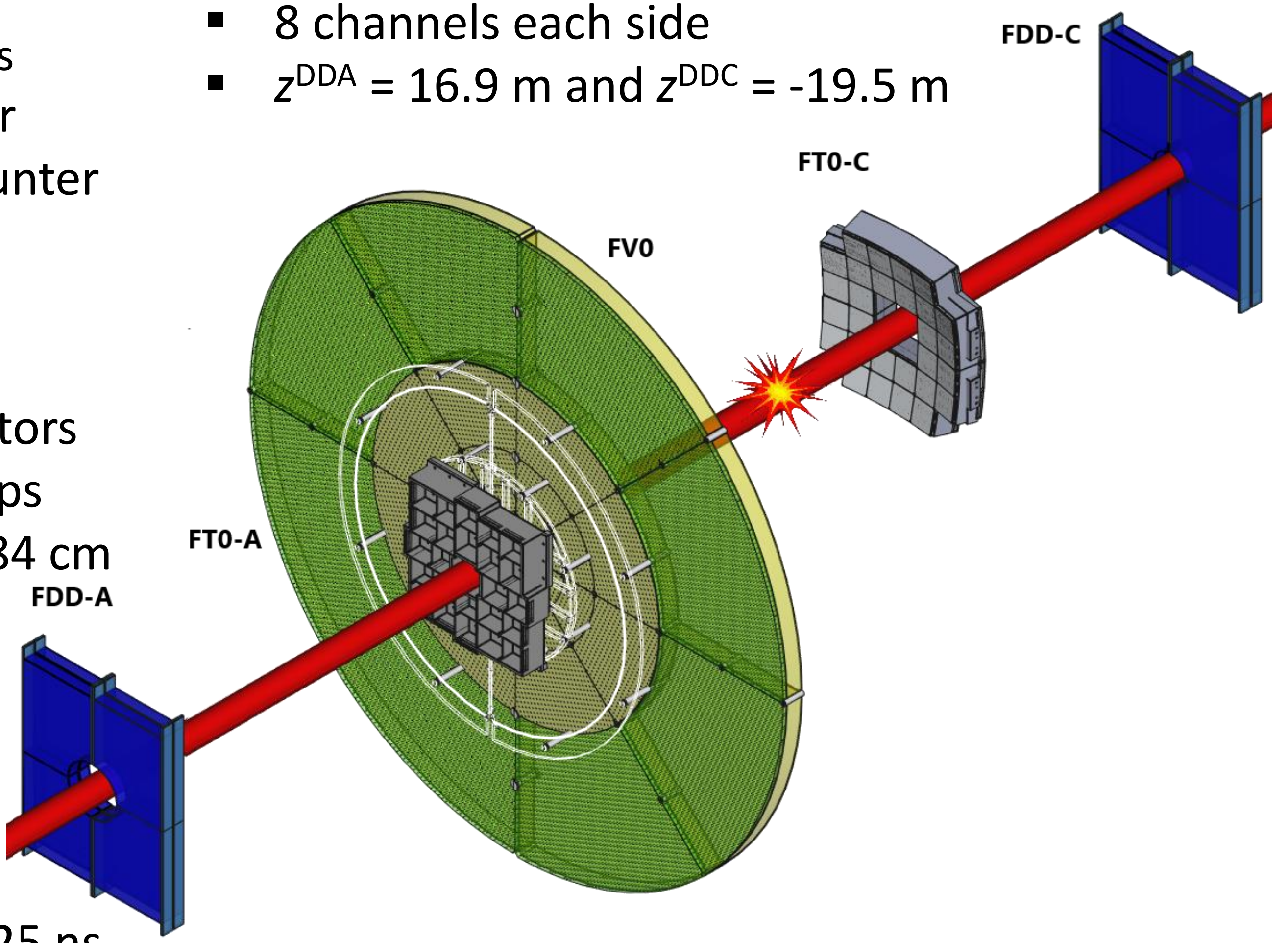

ITS3 in Run 4

- Replacement of 3 most inner layers
- Curved wafer-scale ultra-thin silicon sensors arranged in perfectly cylindrical layers
  - Removal of mechanical suport
  - Homogeneous material distribution
- Extremely low material budget 0.05% X_0 per layer
  - Power and data buses integrated on chip
- Power consumption ~ 20 mW/cm^2
  - Removal of water cooling

⇒ Improved tracking precision and efficiency at low p_T

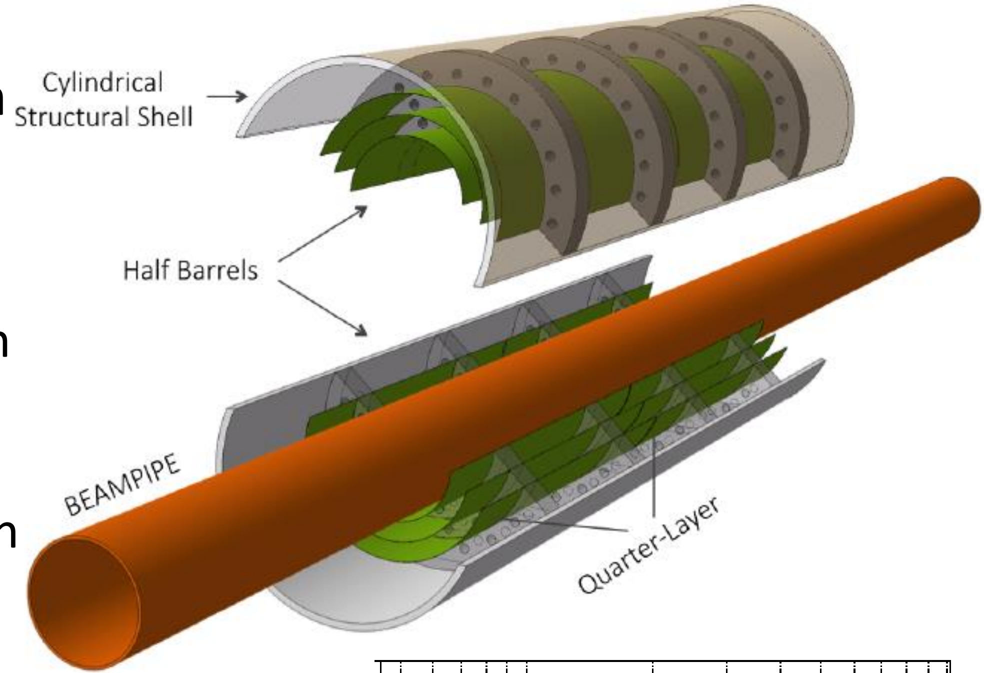

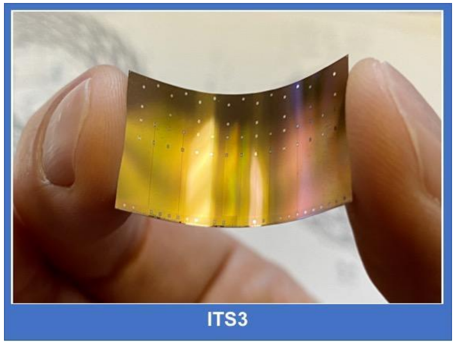

Layer	R_{min} [mm]	η
Beam pipe	16	
0	18	± 2.5
1	24	± 2.3
2	30	± 2.0

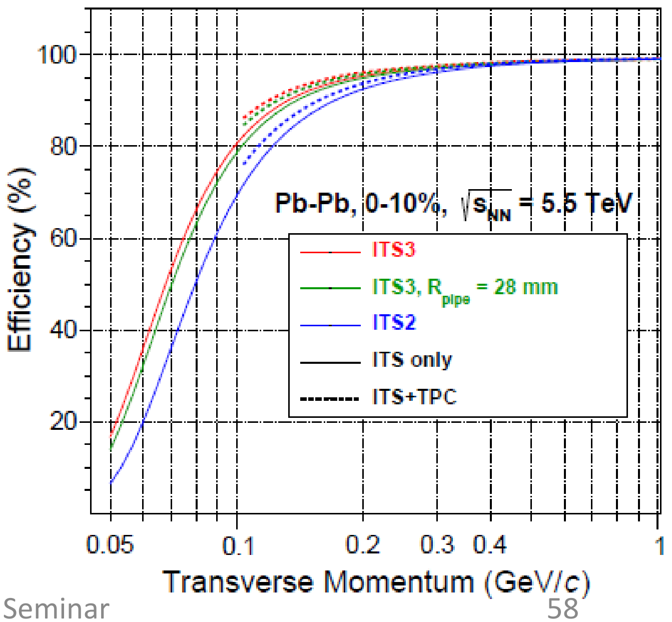

ALICE 3 design

- Retractable vertex detector
  - Detector into beam pipe (R^{in} = 16 → 5 mm)
- All silicon tracker (12 tracking layers + discs based on MAPS)
  - Power consumption ~ 70 mW/cm^2
  - Inner tracker:
    - Ultra thin – flexible wafer scale sensors (MAPS) – X/X_0 ~ 0.01%/layer
    - Position resolution ~1 μm
  - Outer tracker:
    - Low material budget X/X_0 ~ 1%/layer ⇒ low weight suport and services
    - Position resolution ~10 μm
- Particle ID systems (TOF, Cherenkov, EM shower, muon ID, forward detector for soft photons)
  - TOF resolution < 20 ps challenging and material budget X/X_0 ~ 1-3%/layer and power consumption ~ 50 mW/cm^2 and large area (~ 45 m^2)
- Large acceptance $\Delta\eta \sim 9$
- Continuous readout
- Superconducting magnet

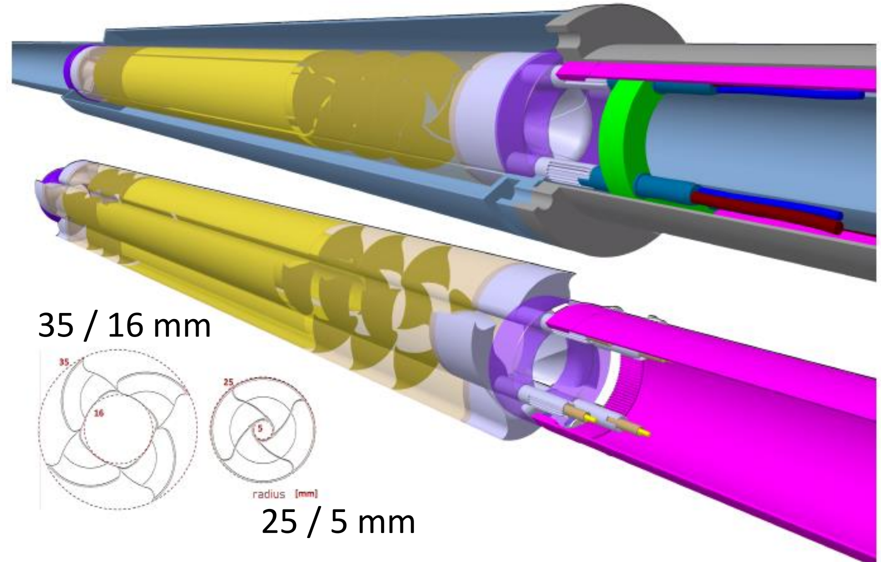

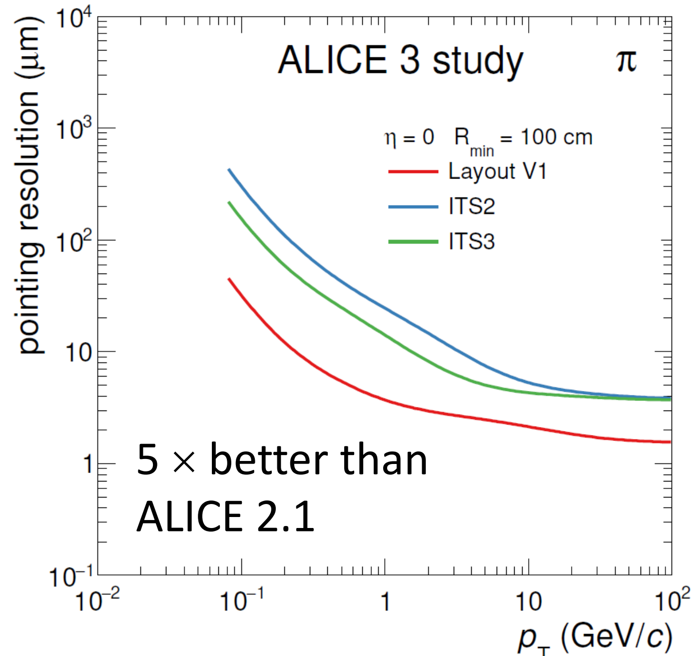

ALICE3 LOI: CERN-LHCC-2022-009 / LHCC-I-038

Anomalous magnetic moment – cont.

- For electrons:
  - $a_e^{exp} = 115\,965\,218\,076\,(28) \times 10^{-14}$ (PDG22)
  - $a_e^{th} = 115\,965\,218\,164.3\,(76.4) \times 10^{-14}$ (T. Aoyama et al., PRD. 91 (3): 033006)

    $\Rightarrow$ 2.5 σ discrepancy
  - Contribution to a_e from particles heavier than electrons is $\sim 4 \times 10^{-12}$

    $\Rightarrow$ Not so sensitive to BSM particles
  - $(m_\mu/m_e)^2 \approx 40000 \Rightarrow a_\mu$ is 40000 $\times$ more sensitive to new physics ($\delta a_l \sim m_l^2/M_S^2$) ; M_S – supersymmetry scale
- For muons:
  - $a_\mu^{exp} = 116\,592\,061 \pm 41 \times 10^{-11}$ (PDG22)
  - $a_\mu^{SM} = 116\,591\,810 \pm 43 \times 10^{-11}$ (0.37 ppm) (T. Aoyama et al., Phys. Rept. 887, 1(2020))
  - $\Rightarrow$ 4.2 σ discrepancy
  - $(m_\tau/m_\mu)^2 \approx 280 \Rightarrow a_\tau$ is 280 $\times$ more sensitive to new physics

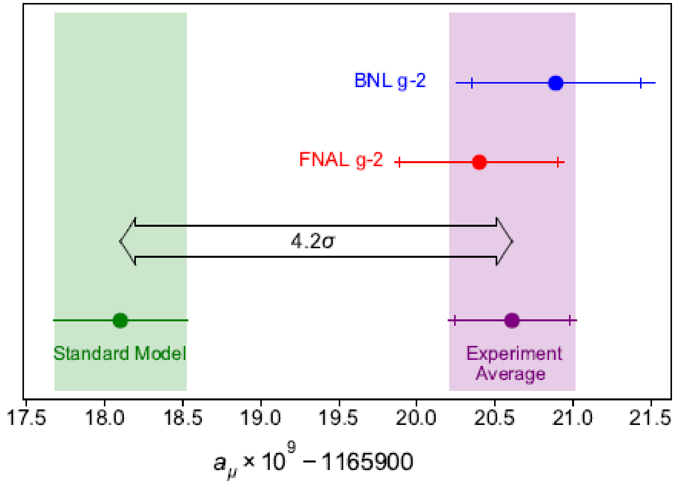

T. Aoyama et al., Phys. Rept. 887, 1(2020)

τ anomalous magnetic moment

- Anomalous magnetic moment:
  - $a_\tau^{exp} = -0.018(17)$ (DELPHI, EPJC 35 (2004) 159)
  - $a_\tau^{SM} = 0.00117721(5)$ (S. Eidelman and M. Passera, Mod. Phys. Lett. A 22, 159 (2007))
- Cross section and τ kinematics sensitive to a_τ
  - L. Beresford and J. Liu, PRD 102 (2020) 113008
  - M. Dyndał et al., PLB 809 (2020) 135682
  - Burmasov et al., arXiv:2203.00990 (2022)

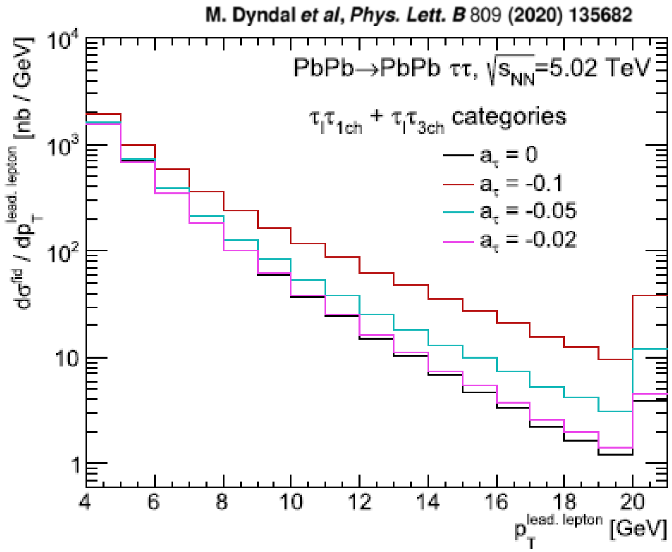

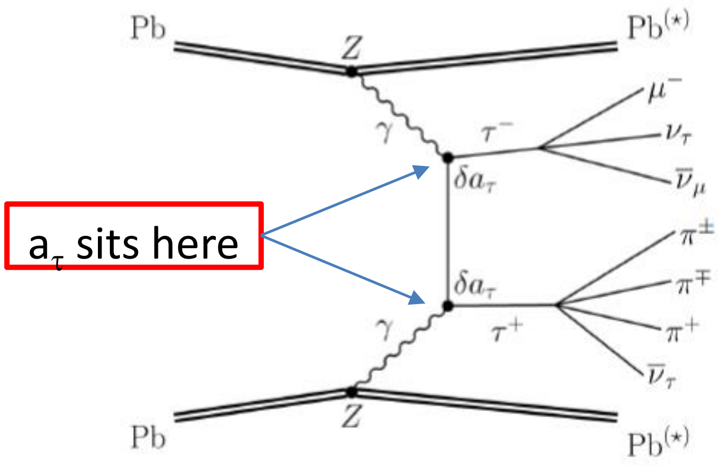

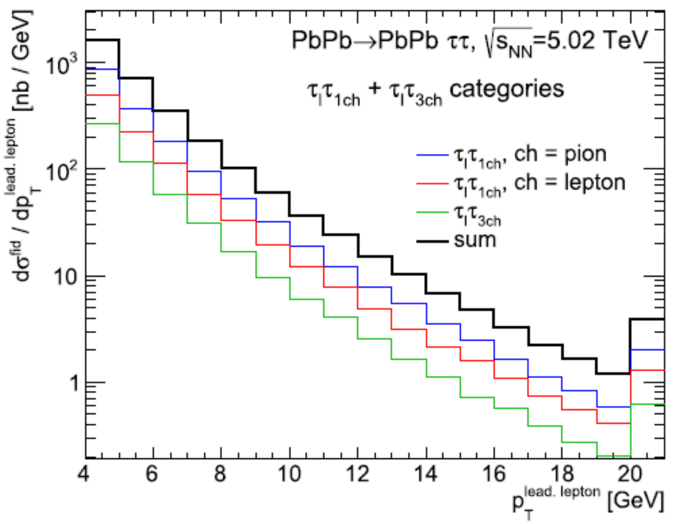

Background description

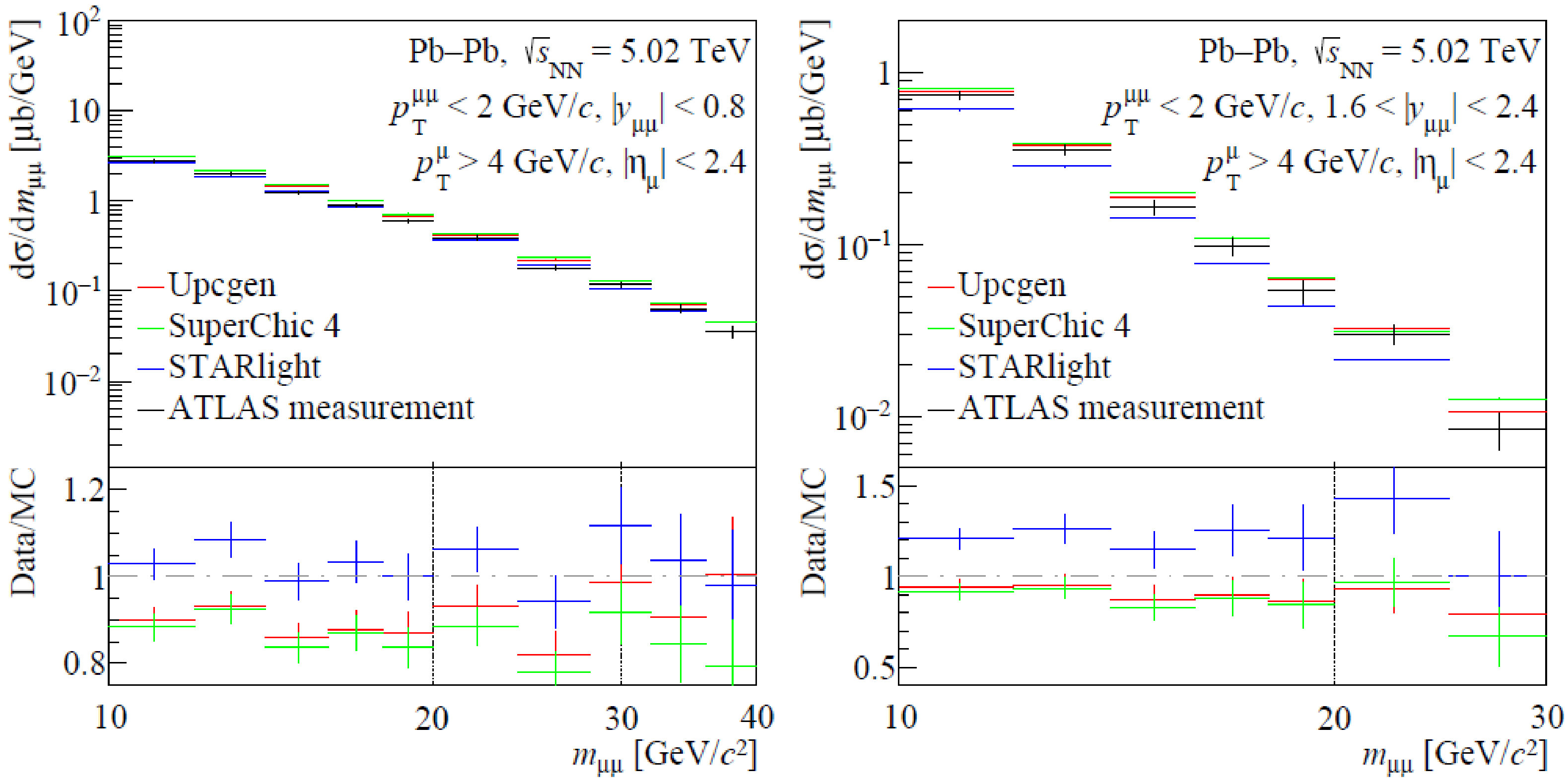

Burmasov et al., 2203.00990 (2022)

- Good description of background processes by MC generators:
  - UPCgen (Burmasov et al., arXiv:2111.11383 (2022))
  - STARlight (Klein et al., Comput. Phys. Commun. 212 (2017))
  - SuperChic (Harland-Lang et al., EPJ C80 (2020))

Measurement of τ pair production

- CMS observation shown at QM2022

CMS-PAS-HIN-21-009

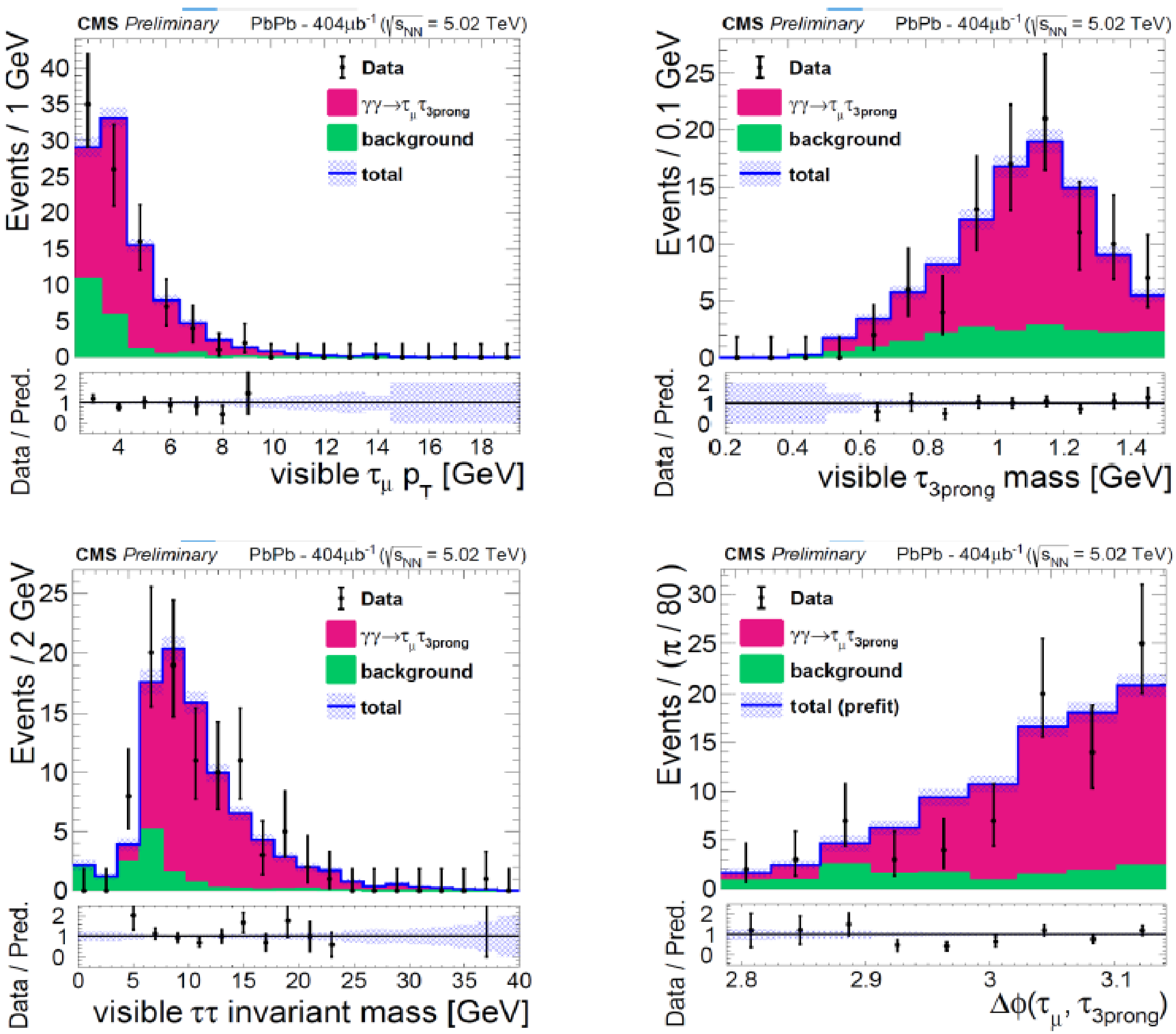

- μ + 3tracks topology
- N_{sig} = 77 ± 12
- L = 404 μb^{-1}

- Good agreement between MC and data
- Only 1+3 topology
- Only μ
- Not full statistics

Measurement of τ pair production

- ATLAS observations shown at QM2022

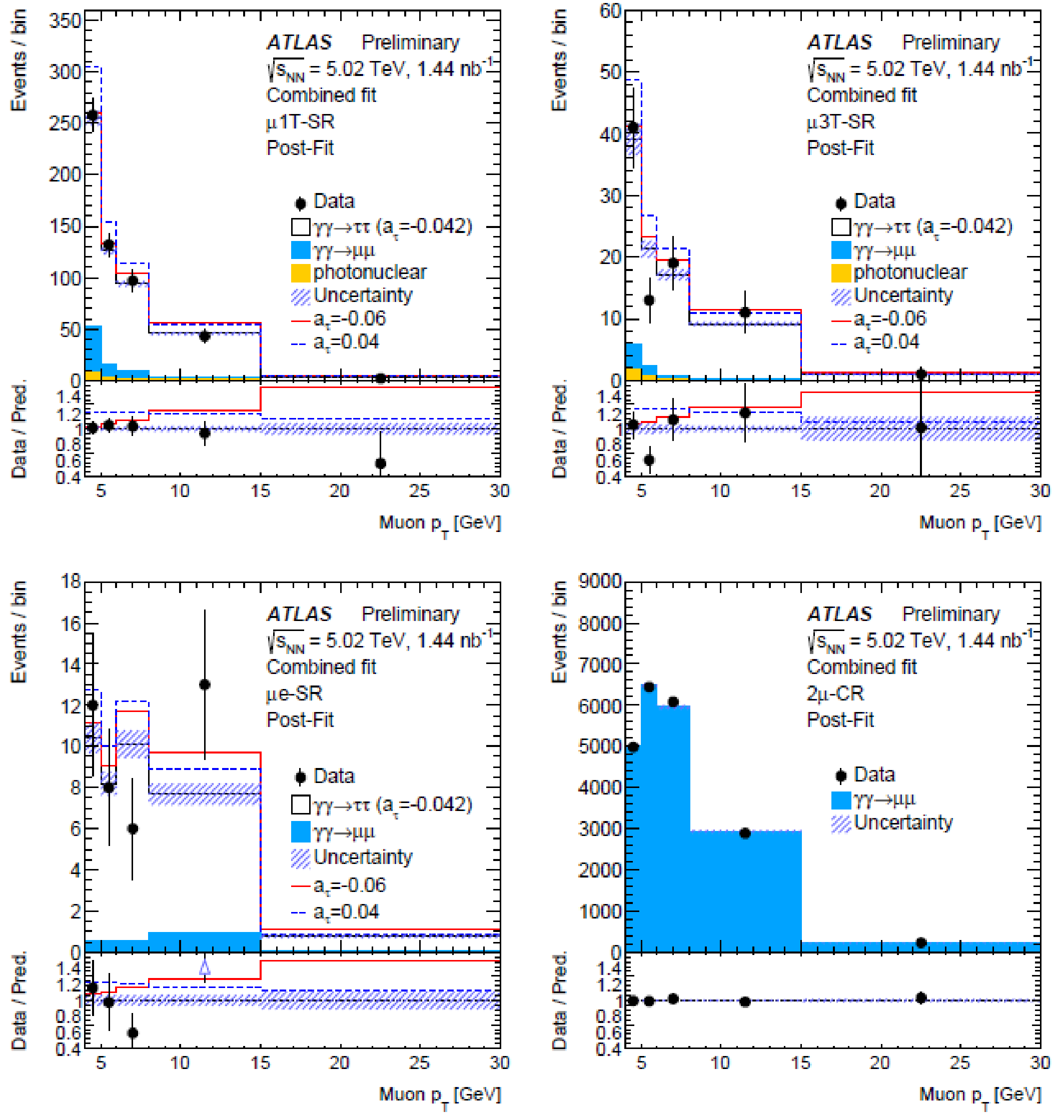

arXiv:2204.13478v1

- μ1T-SR: muon + 1 track (e/μ/hadron)
- μ3T-SR: muon + 3 tracks (3 hadrons)
- μe-SR: muon + electron

N_{sig} = 532, 85 and 39

L = 1.44 / nb

- Good agreement between MC and data
- Several topologies with μ
- Not full statistics

Cross-section predictions

PRL 12 (2016) 129901

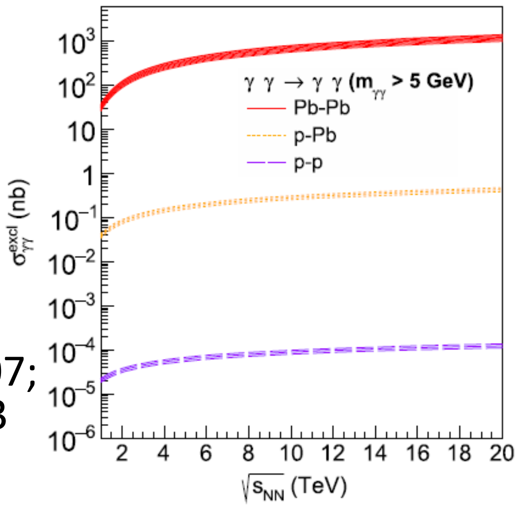

- Calculations of cross-section at the LHC energies:
  - d'Enterria group:
    - d'Enterria, Silveira, PRL 111 (2013) 080405 + Erratum PRL 12 (2016) 129901.
    - High $W_{\gamma\gamma} > 5$ GeV/c^2
  - Kraków group:
    - Kłusek-Gawenda, Lebiedowicz, Szczurek, PRC 93 (2016) 044907; Kłusek-Gawenda, McNulty, Schicker, Szczurek, PRD 99, 093013 (2019)
    - Includes resonances contribution
    - Both high ($W_{\gamma\gamma} > 5$ GeV/c^2) and low ($W_{\gamma\gamma} < 5$ GeV/c^2) masses
    - ALICE and LHCb acceptance
- MC generators:
  - SuperChic 4 (Durham group):
    - Paper - EPJ C 79 (2019) 39
    - Code - https://superchic.hepforge.org/
  - gamma-UPC (d'Enterria et al.):
    - Paper - https://arxiv.org/abs/2207.03012
    - Code - http://cern.ch/hshao/gammaupc.html

PRD 99, 093013 (2019)

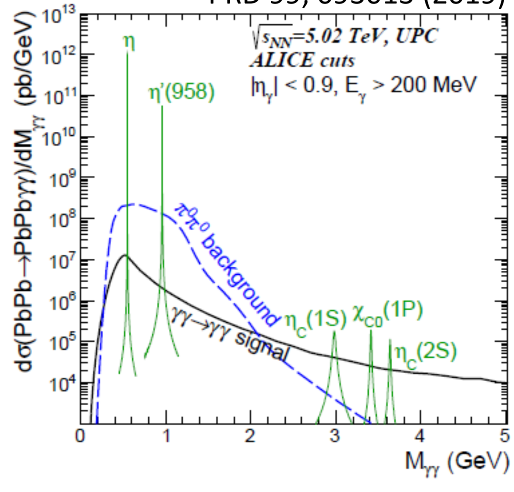

Background sources

- 3 regimes:
  - $W_{\gamma\gamma} > 5$ GeV/c^2 – perturbative, well-known region
  - $2 < W_{\gamma\gamma} < 5$ GeV/c^2
  - $W_{\gamma\gamma} < 2$ GeV/c^2 – non-pertubative, not explored
- Background types
  - Central exclusive production (CEP)
  - (CE) Meson pair production ($\pi^0\pi^0$, $\eta\eta$, $\eta\eta'$, $\eta'\eta'$, …)
  - Combinatorial $\gamma\gamma$ from vector meson photoproduction ($\omega \to \pi^0\gamma \to \gamma\gamma\gamma$, $J/\psi \to \eta_c\gamma$, …)
  - Exclusive dielectron production $\gamma\gamma \to e^+e^-$
  - Hard bremsstrahlung photons emitted by electrons

CEP

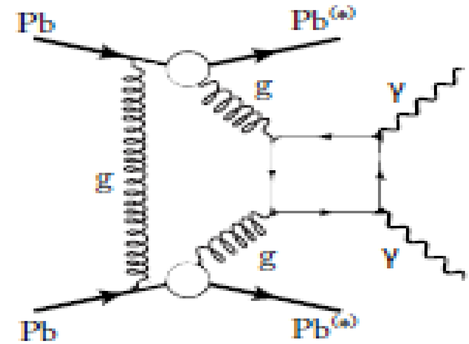

PLB 797 (2019) 134826

Meson pair production

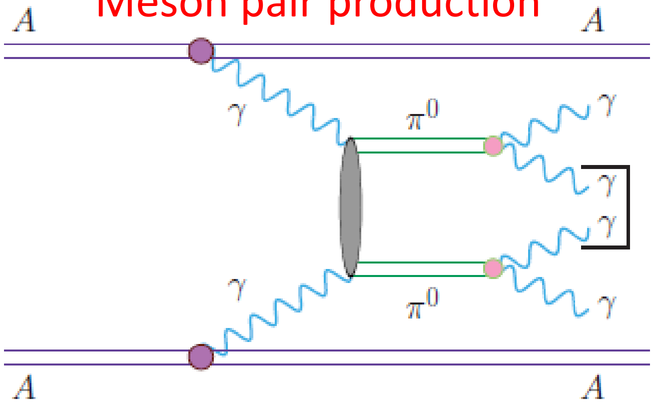

PRD 99, 093013 (2019)

Dielectron production

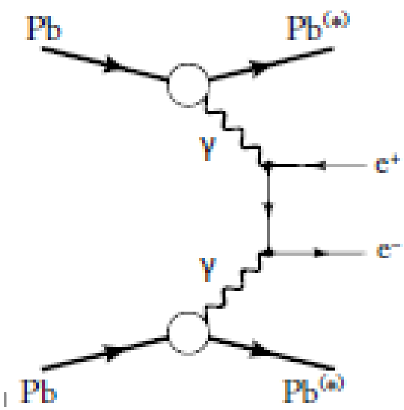

PLB 797 (2019) 134826

Measurements

ATLAS: JHEP 03 (2021) 243

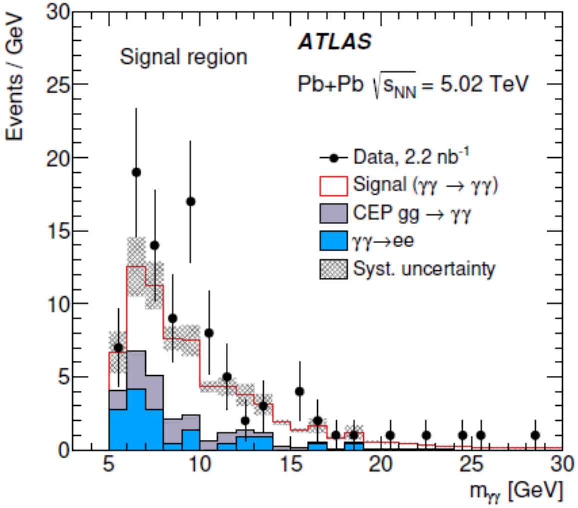

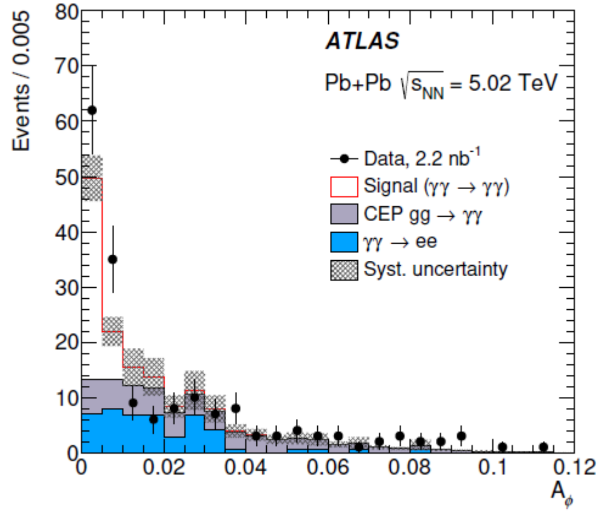

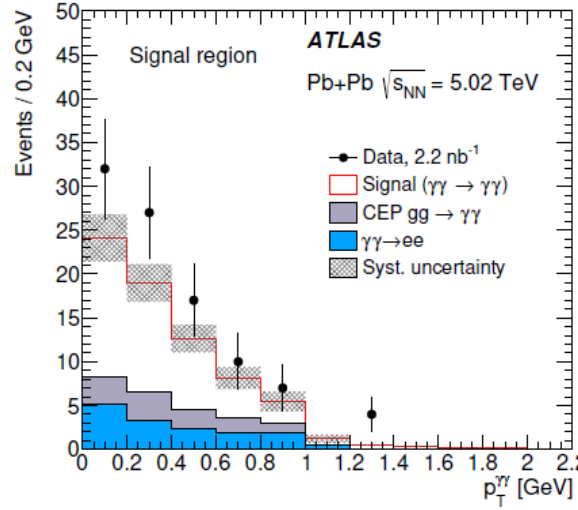

- $E_T^{\gamma} > 2.5$ GeV
- $|\eta_\gamma| < 2.4$
- $N_\gamma = 2$
- $W_{\gamma\gamma} > 5$ GeV/c^2
- Charged particle track veto to suppress $\gamma\gamma \to e^+e^-$
- $p_T^{\gamma\gamma} < 1$ GeV/c for $W_{\gamma\gamma} < 12$ GeV/c^2 or $p_T^{\gamma\gamma} < 2$ GeV/c for $W_{\gamma\gamma} > 12$ GeV/c^2 to reduce fake photons
- Acoplanarity $A_\phi = (1-|\Delta\phi_{\gamma\gamma}|/\pi) < 0.01$ to reduce CEP gg $\to \gamma\gamma$
- Efficiency factor $C^{\text{ATLAS}} = 0.35 \pm 0.024$

Data/Theory comparison

- Measurements at LHC:
  - ATLAS (Nature Phys. 13(2017) 852-858; PRL 123, 052001 (2019); JHEP 03 (2021) 243)
  - CMS (PLB 797 (2019) 134826)

Experiment	N_{events}	Cross-section [nb]	significance	$W_{\gamma\gamma}$ [GeV/c^2]
ATLAS (480 μb^{-1})	13	70 ± 24 (stat) ± 17 (syst)	4.4 σ	> 6
CMS (390 μb^{-1})	14	120 ± 46 (stat) ± 28 (syst) ± 12 (theo)	3.7 σ	> 5
ATLAS (1.73 nb^{-1})	59	78 ± 13 (stat) ± 7 (syst) ± 9 (lumi)	8.2 σ	> 6
ATLAS (2.2 nb^{-1})	97	120 ± 17 (stat) ± 13 (syst) ± 4 (lumi)		> 5

- Theory calculations at LHC:

Group	Cross-section [nb]	$W_{\gamma\gamma}$ [GeV/c^2]
d'Enterria et al.	45 ± 9	> 6
Kraków	51 ± 5	> 6
SuperChic	50 ± 5	> 6

Less than 2σ discrepancy

Data-to-theory ratio:

- 1.50 ± 0.32 (ATLAS – Kraków)
- 1.54 ± 0.32 (ATLAS – SuperChic)

ALICE can provide complementary result in low $W_{\gamma\gamma} < 5$ GeV/c^2

Search for axion-like particles (ALPs)

- Light-by-light scattering is sensitive for BSM physics
- ALPs are class of hypothetical pseudoscalar particles with unknown mass-coupling relation
- Dark matter candidates
- Axions initially proposed to solve CP problem

$$\mathcal{L} = \frac{1}{2}\partial^{\mu} a \partial_{\mu} a - \frac{1}{2} m_a^2 a^2 - \frac{1}{4} g_{a\gamma} a F^{\mu\nu} \tilde{F}_{\mu\nu}$$

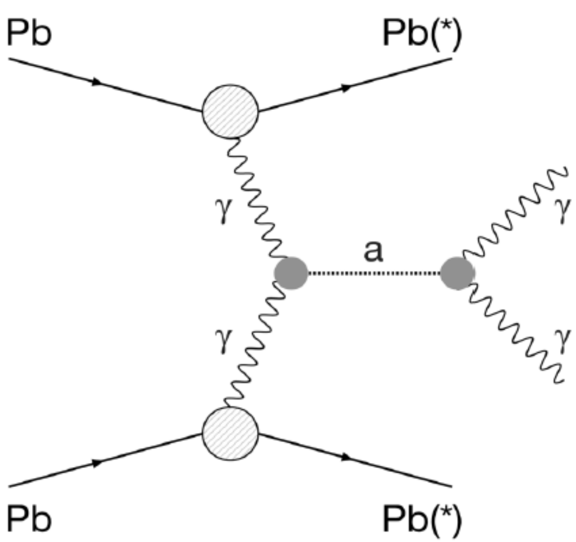

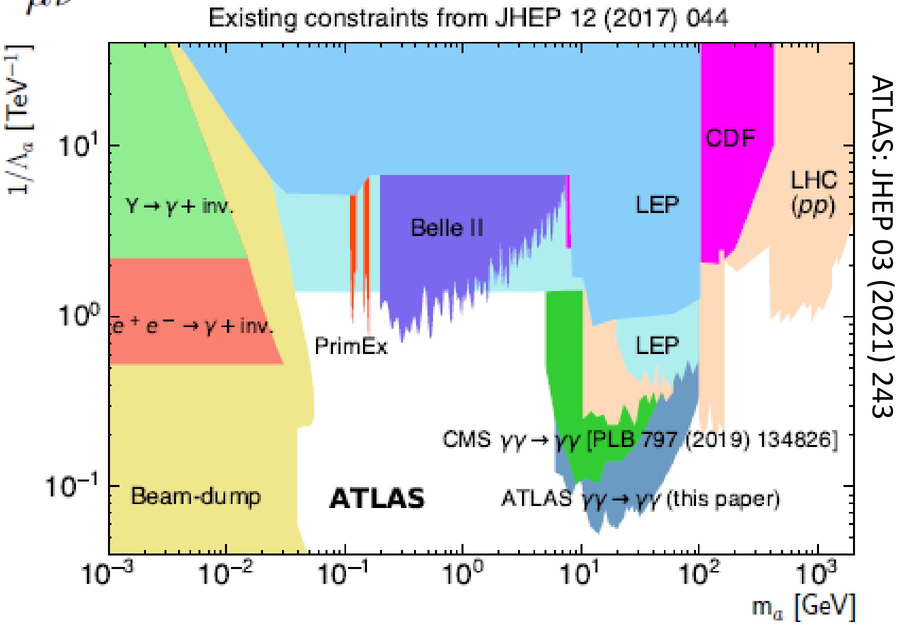

ATLAS and CMS set limits in a mass range $5 < m_a < 100$ GeV/c^2

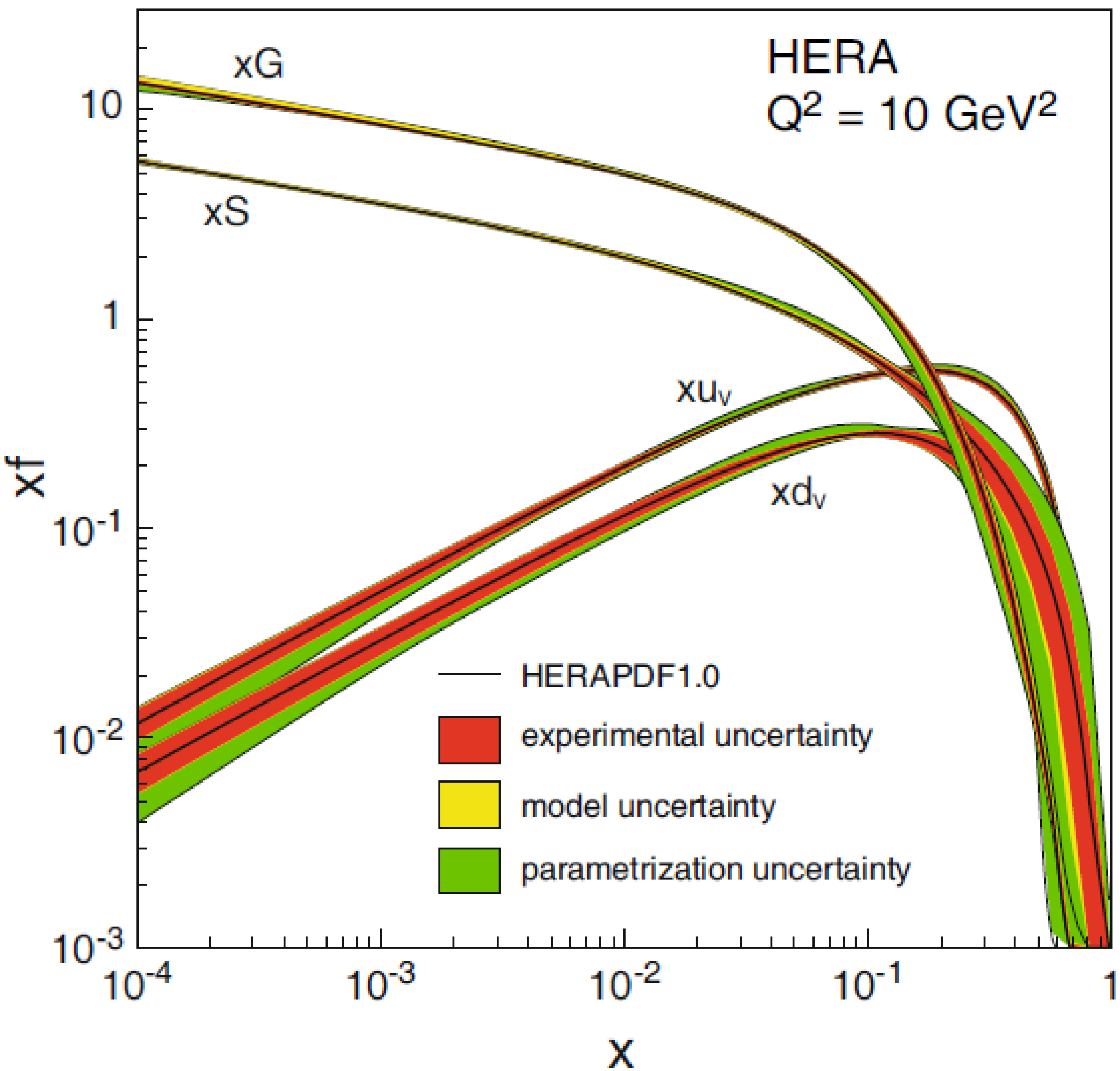
xG
xS
HERA
Q2 = 10 GeV2
xuv
xdv
xf
x
10
1
10-1
10-2
10-3
10-4
10-3
10-2
10-1
1
HERAPDF1.0
experimental uncertainty
model uncertainty
parametrization uncertainty

- DGLAP: Dokshitzer–Gribov–Lipatov–Altarelli–Parisi evolution equations
- BFKL:
  - E.A. Kuraev, L.N. Lipatov and V.S. Fadin, Sov. Phys. JETP 45 (1977), 199;
  - Ya.Ya. Balitsky and L.N. Lipatov, Sov. J. Nucl. Phys. 28 (1978), 22.
- JIMWLK: Jalilian-Marian, Iancu, McLerran, Weigert, Leonidov and Kovner
  - [1] I. Balitsky, “Operator expansion for high-energy scattering”, Nucl. Phys. B 463, 99 (1996)
  - [2] J. Jalilian-Marian, A. Kovner, A. Leonidov and H. Weigert, “The BFKL equation from the Wilson renormalization group”, Nucl. Phys. B 504, 415 (1997)
  - [3] J. Jalilian-Marian, A. Kovner, A. Leonidov and H. Weigert, “The Wilson renormalizationgroup for low x physics: Towards the high density regime”, Phys. Rev. D 59, 014014 (1998)
  - [4] J. Jalilian-Marian, A. Kovner and H. Weigert, “The Wilson renormalization group for low x physics: Gluon evolution at finite parton density”, Phys. Rev. D 59, 014015 (1998)
  - [5] A. Kovner, J. G. Milhano and H. Weigert, “Relating different approaches to nonlinear QCD evolution at finite gluon density”, Phys. Rev. D 62, 114005 (2000)
  - **[6] E. Iancu, A. Leonidov and L. D. McLerran, “Nonlinear gluon evolution in the color glass condensate. 1”, Nucl. Phys. A 692, 583 (2001)**
  - [7] E. Ferreiro, E. Iancu, A. Leonidov and L. McLerran, “Nonlinear gluon evolution in the color glass condensate. 2”, Nucl. Phys. A 703, 489 (2002)
  - [8] A. H. Mueller, “A Simple derivation of the JIMWLK equation”, Phys. Lett. B 523, 243 (2001)